CHAPTER 1

NMR Consequences of the Nucleus–Electron Spin Interactions

GIACOMO PARIGI[a,b] AND CLAUDIO LUCHINAT*[a,b]

[a] Magnetic Resonance Center (CERM), via L. Sacconi 6, Sesto Fiorentino 50019, Italy; [b] Department of Chemistry ''Ugo Schiff'', University of Florence, via della Lastruccia 3, Sesto Fiorentino 50019, Italy
*Email: claudioluchinat@cerm.unifi.it

1.1 The Effect of Paramagnetism on NMR Spectra

The presence of unpaired electrons in molecules makes them paramagnetic and largely affects their NMR spectra. The main effects related to the presence of a paramagnetic center, *i.e.*, of atoms or ions with unpaired electrons, are (see Figure 1.1):[1]

(1) the NMR shifts are perturbed, so that the shifts measured for the paramagnetic molecule (δ) and for a diamagnetic analogue (δ^{dia}) (*i.e.*, for the same molecule without the paramagnetic center or with the paramagnetic metal ion substituted by a diamagnetic one) differ. These differences are called hyperfine shifts (δ^{hs}):

$$\delta = \delta^{dia} + \delta^{hs} \tag{1.1}$$

(2) the nuclear relaxation rates of the paramagnetic molecule (R_1, longitudinal; R_2, transverse) are increased with respect to those of a

New Developments in NMR No. 16
Paramagnetism in Experimental Biomolecular NMR
Edited by Claudio Luchinat, Giacomo Parigi and Enrico Ravera

Published by the Royal Society of Chemistry, www.rsc.org

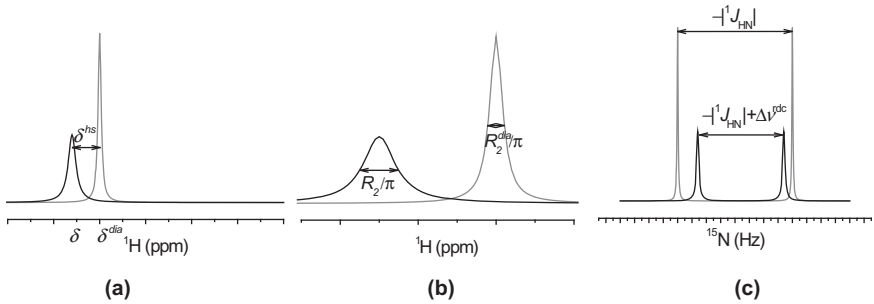

Figure 1.1 The presence of a paramagnetic center affects NMR shifts (a), relaxation rates (b) and ^1J splitting (c).

diamagnetic analogue (R_1^{dia} and R_2^{dia}). This difference is called paramagnetic relaxation enhancement (R_{1M} and R_{2M}):

$$R_1 = R_1^{\mathrm{dia}} + R_{1M},\ R_2 = R_2^{\mathrm{dia}} + R_{2M} \tag{1.2}$$

(3) the probabilities for the different orientations of the paramagnetic molecule in a magnetic field are not the same, so a partial self-orientation occurs. This partial self-orientation is responsible for the occurrence of residual dipolar couplings ($\Delta\nu^{\mathrm{rdc}}$), analogously to what happens when partial molecular orientation is driven by external devices. The presence of paramagnetic residual dipolar couplings affects the *J*-coupling between nuclei:

$$^1J_{12}\,(B_0) = {}^1J_{12} + \Delta\nu^{\mathrm{dia}} + \Delta\nu^{\mathrm{rdc}} \tag{1.3}$$

This chapter deals with the description of these effects, and of their physical origin, which is related to the so-called hyperfine coupling. In eqn (1.1)–(1.3) other minor effects, namely residual anisotropic chemical shifts, cross relaxation terms, and dynamic frequency shifts, respectively, have been neglected (see later).

1.1.1 The Hyperfine Coupling

The interaction between the magnetic moment associated to a nuclear spin **I** and the magnetic moment associated to an unpaired electron spin **S** is called hyperfine coupling and is traditionally described by the Hamiltonian

$$H_{\mathrm{hc}} = \mathbf{S} \cdot \mathbf{A} \cdot \mathbf{I} \tag{1.4}$$

The energy corresponding to this interaction fluctuates with time (and thus this interaction represents a source of relaxation for the nuclear spin, see Section 1.4) as a result of the molecular motions and of changes in the

electron spin state. The other terms describing the contributions to the energy of the system are:

(i) the Zeeman interaction between the applied magnetic field $\mathbf{B_0}$ and the nuclear magnetic moment $\boldsymbol{\mu}_\mathbf{I} = \hbar\gamma_I\mathbf{I}$, where $\hbar$ is Planck's constant divided by 2π and γ_I is the nuclear magnetogyric ratio,
(ii) the Zeeman interaction between $\mathbf{B_0}$ and an 'effective' electron magnetic moment taking into account both the electron spin and the orbital magnetic moments. This is parameterised using the $\mathbf{g}$ tensor, with the effective electron magnetic moment given by $\boldsymbol{\mu}_\mathbf{S} = -\mu_\mathrm{B}\mathbf{g}\cdot\mathbf{S}$, where μ_B is the electron Bohr magneton. Therefore, the $\mathbf{g}$ tensor couples the 'effective' electron spin to $\mathbf{B_0}$, thus accounting for the presence of the anisotropic orbital contributions to the electron magnetic moment. As a result, the latter depends on the orientation of the molecule with respect to the magnetic field direction,
(iii) the zero-field splitting (ZFS) interaction, due to the spin–orbit coupling, for systems with more than one unpaired electron ($S > 1/2$), and
(iv) all other diamagnetic interactions present in the molecule.

The whole Hamiltonian describing a paramagnetic system is thus composed of the terms

$$H = -\hbar\gamma_I\mathbf{B_0}\cdot\mathbf{I} + \mu_\mathrm{B}\mathbf{B_0}\cdot\mathbf{g}\cdot\mathbf{S} + \mathbf{S}\cdot\mathbf{D}\cdot\mathbf{S} + H_\mathrm{dia} + H_\mathrm{hc} \tag{1.5}$$

where $\mathbf{D}$ is the ZFS tensor.

The $\mathbf{A}$ tensor in H_hc is composed of two terms: the isotropic Fermi-contact term and the anisotropic electron–nucleus dipole–dipole interaction term

$$\mathbf{A} = A^\mathrm{FC}\mathbf{1} + \mathbf{A^{DIP}} \tag{1.6}$$

where A^FC is a scalar and $\mathbf{A^{DIP}}$ is a traceless symmetric tensor. The scalar term, called the contact coupling constant, is given by

$$A^\mathrm{FC} = \frac{\mu_0}{3S}\hbar\gamma_I g_\mathrm{e}\mu_\mathrm{B}\rho \tag{1.7}$$

where μ_0 is the permeability of the vacuum, g_e is the free-electron g factor and ρ is the electron spin density at the nucleus (normalized to one electron). Anisotropic orbital contributions are excluded from A^FC because the coupling responsible for the contact interaction is only with the unpaired electron spin density residing on the nucleus (and thus in s orbitals).

In the point-dipole approximation (see Section 1.2.2), the dipolar term $\mathbf{S}\cdot\mathbf{A^{DIP}}\cdot\mathbf{I}$ should describe the energy related to the dipolar magnetic

field generated by the magnetic moments, which, in the classical approach, is[2]

$$E^{\mathrm{DIP}} = -\frac{\mu_0}{4\pi r^3}\boldsymbol{\mu}_{\mathbf{S}} \cdot \left(\frac{3\mathbf{rr}}{r^2} - \mathbf{1}\right) \cdot \boldsymbol{\mu}_{\mathbf{I}} = \frac{\mu_0}{4\pi}\frac{\hbar\gamma_I\mu_{\mathrm{B}}}{r^5}\mathbf{S} \cdot \mathbf{g}^T \cdot \begin{pmatrix} 3x^2 - r^2 & 3xy & 3xz \\ 3xy & 3y^2 - r^2 & 3yz \\ 3xz & 3yz & 3z^2 - r^2 \end{pmatrix} \cdot \mathbf{I} \tag{1.8}$$

where the effective electron magnetic moment is considered to take into account the presence of the orbital contributions. Therefore,

$$\mathbf{A}^{\mathbf{DIP}} = \frac{\mu_0}{4\pi}\frac{\hbar\gamma_I\mu_{\mathrm{B}}}{r^3}\mathbf{g}^T \cdot \left(\frac{3\mathbf{rr}}{r^2} - \mathbf{1}\right) \tag{1.9}$$

where the superscript T indicates the matrix transpose, and $\mathbf{r}$ is the vector connecting the positions of the nuclear and electron spins. Of note, the components of the $\mathbf{g}$ tensor are not the experimental EPR values obtained for the ground state, but the molecular g values along the main directions of the tensor.

In quantum chemistry computations, a different formulation for the $\mathbf{A}^{\mathbf{DIP}}$ tensor is used (see Section 1.6).

1.1.2 The Curie Spin

The tiny difference in population between the nuclear spin states in the presence of a magnetic field, at room temperature, is responsible for the NMR signal originated by that nucleus. In fact, this difference causes an induced average magnetic moment, which is proportional to the observed NMR signal (see Section 8.1.1). The larger the magnetic field (and the smaller the temperature), the larger the difference in spin population, and thus the induced average magnetic moment.

The difference in population between the different spin states is much larger for electrons than for protons, due to their larger magnetogyric ratio ($\gamma_S/\gamma_{\mathrm{H}} = 658.2$). This difference is also of paramount importance for the understanding of the NMR spectra of paramagnetic systems. The electron spin $\mathbf{S}$ is thus conveniently separated into two terms, corresponding to the null average part $\mathbf{s}$ ($\langle\mathbf{s}\rangle = 0$) and to the thermal average of $\mathbf{S}$, $\mathbf{S}_{\mathbf{C}}$:

$$\mathbf{S} = \mathbf{s} + \mathbf{S}_{\mathbf{C}} = \mathbf{s} + \langle S_z\rangle\boldsymbol{\kappa} \tag{1.10}$$

where $\boldsymbol{\kappa}$ is the versor of $\mathbf{S}_{\mathbf{C}}$, which in general differs from the magnetic field direction (see later). Therefore, the electron (thermal average) induced magnetic moment is given by

$$\langle\boldsymbol{\mu}_{\mathbf{S}}\rangle = -\ \mu_{\mathrm{B}}\mathbf{g} \cdot \mathbf{S}_{\mathbf{C}} \tag{1.11}$$

In quantum mechanics formalism the magnetic moment is defined as the partial derivative of the energy with respect to the magnetic field

$$\boldsymbol{\mu} = -\frac{\partial E}{\partial \mathbf{B_0}} \quad \left(\text{meaning } \mu_\alpha = -\frac{\partial E}{\partial B_{0\alpha}},\ \text{with } \alpha = x, y, z\right) \tag{1.12}$$

so that

$$\langle \boldsymbol{\mu}_\mathbf{S} \rangle = -\frac{\sum_i \frac{\partial E_i}{\partial \mathbf{B_0}} \exp[-E_i/(kT)]}{\sum_i \exp[-E_i/(kT)]} \tag{1.13}$$

where E_i is the energy of the electron i-th state, k is the Boltzmann constant and T is the temperature. Following van Vleck, let us suppose that E_i can be written to a good approximation through perturbation theory limited to second-order correction to the ground state energy

$$E_i = E_i^0 + E_i^{(1)} + E_i^{(2)} = E_i^0 + \langle i|H^{(1)}|i\rangle + \sum_{k\neq i} \frac{\left|\langle i|H^{(1)}|k\rangle\right|^2}{E_i^0 - E_k^0} \tag{1.14}$$

In our case $H^{(1)}$ is the Zeeman energy ($H^{(1)} = -\mathbf{B_0} \cdot \boldsymbol{\mu}_\mathbf{S}$), so that $E^{(1)}$ and $E^{(2)}$ for relatively small B_0 are much smaller than the eigenvalues of $H^{(0)}$, E^0, independent of the magnetic field. Therefore,

$$\begin{aligned}
\langle \boldsymbol{\mu}_\mathbf{S} \rangle &= -\frac{\sum_i \frac{\partial (E_i^{(1)} + E_i^{(2)})}{\partial \mathbf{B_0}} \exp[-E_i/(kT)]}{\sum_i \exp[-E_i/(kT)]} \\
&= \frac{\sum_i \frac{\partial \left(\langle i|\mathbf{B_0} \cdot \boldsymbol{\mu}_\mathbf{S}|i\rangle - \sum_{k\neq i} \frac{\left|\langle i|\mathbf{B_0} \cdot \boldsymbol{\mu}_\mathbf{S}|k\rangle\right|^2}{E_i^0 - E_k^0} \right)}{\partial \mathbf{B_0}} \exp[-E_i/(kT)]}{\sum_i \exp[-E_i/(kT)]} \\
&= \frac{\sum_i \left(\langle i|\boldsymbol{\mu}_\mathbf{S}|i\rangle - \sum_{k\neq i} \frac{\langle i|\boldsymbol{\mu}_\mathbf{S}|k\rangle\langle k|\mathbf{B_0} \cdot \boldsymbol{\mu}_\mathbf{S}|i\rangle + \langle i|\mathbf{B_0} \cdot \boldsymbol{\mu}_\mathbf{S}|k\rangle\langle k|\boldsymbol{\mu}_\mathbf{S}|i\rangle}{E_i^0 - E_k^0} \right) \exp[-E_i/(kT)]}{\sum_i \exp[-E_i/(kT)]}
\end{aligned} \tag{1.15}$$

Then, to the first order in $E_i/(kT)$

$$\langle \boldsymbol{\mu}_\mathbf{S} \rangle = \frac{\sum_i \left(\langle i|\boldsymbol{\mu}_\mathbf{S}|i\rangle - \sum_{k\neq i} \frac{2\langle i|\mathbf{B_0} \cdot \boldsymbol{\mu}_\mathbf{S}|k\rangle\langle k|\boldsymbol{\mu}_\mathbf{S}|i\rangle}{E_i^0 - E_k^0} \right) \exp\left[-E_i^0/(kT)\right] \left[1 - E_i^{(1)}/(kT)\right]}{\sum_i \exp\left[-E_i^0/(kT)\right] \left[1 - E_i^{(1)}/(kT)\right]} \tag{1.16}$$

Since $\sum_i \langle i|\boldsymbol{\mu}_S|i\rangle \exp\left[-E_i^0/(kT)\right] = 0$, and retaining only the linear terms in B_0

$$\langle \boldsymbol{\mu}_S \rangle = \frac{\sum_i \left(\langle i|\boldsymbol{\mu}_S|i\rangle \frac{\langle i|\mathbf{B_0}\cdot\boldsymbol{\mu}_S|i\rangle}{kT} - \sum_{k\neq i} \frac{2\langle i|\boldsymbol{\mu}_S|k\rangle\langle k|\mathbf{B_0}\cdot\boldsymbol{\mu}_S|i\rangle}{E_i^0 - E_k^0} \right) \exp\left[-E_i^0/(kT)\right]}{\sum_i \exp\left[-E_i^0/(kT)\right]}$$

$$= \frac{\sum_i \left(\frac{\langle i|\boldsymbol{\mu}_S|i\rangle\langle i|\boldsymbol{\mu}_S|i\rangle}{kT} - \sum_{k\neq i} \frac{2\langle i|\boldsymbol{\mu}_S|k\rangle\langle k|\boldsymbol{\mu}_S|i\rangle}{E_i^0 - E_k^0} \right) \exp\left[-E_i^0/(kT)\right]}{\sum_i \exp\left[-E_i^0/(kT)\right]} \cdot \mathbf{B_0} \tag{1.17}$$

In the second term of the numerator, the average of the values calculated over the i and k states is

$$\frac{1}{2}\left(\frac{\langle i|\boldsymbol{\mu}_S|k\rangle\langle k|\boldsymbol{\mu}_S|i\rangle \exp\left[-E_i^0/(kT)\right]}{E_i^0 - E_k^0} + \frac{\langle k|\boldsymbol{\mu}_S|i\rangle\langle i|\boldsymbol{\mu}_S|k\rangle \exp\left[-E_k^0/(kT)\right]}{E_k^0 - E_i^0} \right)$$

$$= \frac{1}{2}\langle i|\boldsymbol{\mu}_S|k\rangle\langle k|\boldsymbol{\mu}_S|i\rangle \frac{\exp\left[-E_i^0/(kT)\right] - \exp\left[-E_k^0/(kT)\right]}{E_i^0 - E_k^0}$$

so that

$$\langle \boldsymbol{\mu}_S \rangle = \frac{\sum_i \left(\frac{\langle i \mid \boldsymbol{\mu}_S|i\rangle\langle i|\boldsymbol{\mu}_S|i\rangle}{kT} \exp\left[-E_i^0/(kT)\right] - \sum_{k\neq i} \frac{\langle i|\boldsymbol{\mu}_S|k\rangle\langle k|\boldsymbol{\mu}_S|i\rangle}{E_i^0 - E_k^0} \left\{ \exp\left[-E_i^0/(kT)\right] - \exp\left[-E_k^0/(kT)\right] \right\} \right)}{\sum_i \exp\left[-E_i^0/(kT)\right]} \cdot \mathbf{B_0} \tag{1.18}$$

This equation is derived on the assumption that all states at zero field are not degenerate. In the presence of states (indicated by the indexes λ and η) with degeneracy (indicated by n and m),

$$\langle \boldsymbol{\mu}_S \rangle = \frac{\mu_B^2}{kT} \times$$

$$\mathbf{g} \cdot \sum_\lambda \left(\sum_{nm} \langle \lambda, n|\mathbf{S}|\lambda, m\rangle\langle \lambda, m|\mathbf{S}|\lambda, n\rangle \exp[-E_\lambda^0/(kT)] - kT \times \sum_{\eta\neq\lambda} \frac{\sum_{nm} \langle \lambda, n|\mathbf{S}|\eta, m\rangle\langle \eta, m|\mathbf{S}|\lambda, n\rangle \{\exp[-E_\lambda^0/(kT)] - \exp[-E_\eta^0/(kT)]\}}{E_\lambda^0 - E_\eta^0} \right) \cdot \mathbf{g}^T$$

$$\frac{}{\sum_{\lambda,n} \exp\left[-E_\lambda^0/(kT)\right]} \cdot \mathbf{B_0} \tag{1.19}$$

Eqn (1.18) and (1.19) can be written as

$$\langle \boldsymbol{\mu}_{\mathbf{S}} \rangle = \frac{\mu_{\mathrm{B}}^2}{kT} \mathbf{g} \cdot \langle \mathbf{SS} \rangle \cdot \mathbf{g}^T \cdot \mathbf{B_0} \tag{1.20}$$

where $\langle \mathbf{SS} \rangle$ is the effective electron spin dyadic equal to

$$\langle S_i S_j \rangle = \frac{\sum_{mn} Q_{mn} \langle n|S_i|m\rangle \langle m|S_j|n\rangle}{\sum_n \exp\left[-E_n^0/(kT)\right]}, \qquad i,j = \{x,y,z\} \tag{1.21}$$

$$Q_{mn} = \begin{cases} \exp\left[-E_n^0/(kT)\right] & \text{for } E_n^0 = E_m^0 \\ -\dfrac{kT}{E_m^0 - E_n^0}\left\{\exp\left[-E_m^0/(kT)\right] - \exp\left[-E_n^0/(kT)\right]\right\} & \text{for } E_n^0 \neq E_m^0 \end{cases}$$

where E_n^0 is the energy of the state $|n\rangle$ at zero magnetic field.

Using eqn (1.11) and (1.20),

$$\mathbf{S_C} = -\frac{\mu_{\mathrm{B}}}{kT} \langle \mathbf{SS} \rangle \cdot \mathbf{g}^T \cdot \mathbf{B_0} \tag{1.22}$$

Therefore, $\langle \boldsymbol{\mu}_{\mathbf{S}} \rangle$ and $\mathbf{S_C}$ are anisotropic quantities, *i.e.*, they have different values for the different directions of the magnetic field with respect to the molecular frame.

As an example, we can consider the case of an $S = 1$ system with the states $|+1\rangle$ and $|-1\rangle$ higher in energy than the state $|0\rangle$ of a quantity D (axial ZFS). Let us suppose that excited states have energy much larger than kT. Recalling that $S_x = (S_+ + S_-)/2$, $S_y = (S_+ - S_-)/2i$, $S_z|m_s\rangle = m_s|m_s\rangle$ and $S_\pm|m_S\rangle = \sqrt{S(S+1) - m_S(m_S \pm 1)}|m_S \pm 1\rangle$, the non-null elements of $\langle \mathbf{SS} \rangle$ are:

$$\langle S_x S_x \rangle = \langle S_y S_y \rangle = \frac{2kT}{D} \frac{1 - \exp\left(-\dfrac{D}{kT}\right)}{2\exp\left(-\dfrac{D}{kT}\right) + 1}, \quad \langle S_z S_z \rangle = \frac{2\exp\left(-\dfrac{D}{kT}\right)}{2\exp\left(-\dfrac{D}{kT}\right) + 1}$$

and thus

$$\mathbf{S_C} = -\frac{\mu_{\mathrm{B}}}{kT} \times \begin{pmatrix} \dfrac{2kT}{D} \dfrac{1 - \exp\left(-\dfrac{D}{kT}\right)}{2\exp\left(-\dfrac{D}{kT}\right) + 1} & 0 & 0 \\ 0 & \dfrac{2kT}{D} \dfrac{1 - \exp\left(-\dfrac{D}{kT}\right)}{2\exp\left(-\dfrac{D}{kT}\right) + 1} & 0 \\ 0 & 0 & \dfrac{2\exp\left(-\dfrac{D}{kT}\right)}{2\exp\left(-\dfrac{D}{kT}\right) + 1} \end{pmatrix}$$

$$\times \begin{pmatrix} g_{xx} & 0 & 0 \\ 0 & g_{yy} & 0 \\ 0 & 0 & g_{zz} \end{pmatrix} \begin{pmatrix} B_x \\ B_y \\ B_z \end{pmatrix} = -\frac{\mu_B}{kT} \begin{pmatrix} g_{xx}\frac{2kT}{D}\frac{1-\exp\left(-\frac{D}{kT}\right)}{2\exp\left(-\frac{D}{kT}\right)+1}B_x \\ g_{yy}\frac{2kT}{D}\frac{1-\exp\left(-\frac{D}{kT}\right)}{2\exp\left(-\frac{D}{kT}\right)+1}B_y \\ g_{zz}\frac{2\exp\left(-\frac{D}{kT}\right)}{2\exp\left(-\frac{D}{kT}\right)+1}B_z \end{pmatrix} \quad (1.23)$$

1.1.3 The Magnetic Susceptibility

As we have seen, a magnetic field induces magnetic moments with non-null thermal average (eqn (1.20)). Usually, the larger the field, the larger the magnetization (until saturation conditions are met). The magnetic susceptibility is defined as the derivative of the magnetization of a substance with respect to the magnetic field strength; if the magnetic field is weak enough not to reach the saturation conditions and thus the magnetization increases linearly with $\mathbf{B_0}$, the magnetic susceptibility is independent of the magnetic field strength. In paramagnetic systems, the magnetization is determined by the induced electron magnetic moments; therefore,

$$\boldsymbol{\chi} = \mu_0 \frac{\partial \langle \boldsymbol{\mu}_\mathbf{S} \rangle}{\partial \mathbf{B_0}} \quad \left(\text{meaning } \chi_{\alpha\beta} = \mu_0 \frac{\partial \langle \mu_{S\alpha} \rangle}{\partial B_{0\beta}}, \text{with } \alpha, \beta = x, y, z \right) \quad (1.24)$$

and thus (using eqn (1.20))

$$\boldsymbol{\chi} = \frac{\mu_0 \mu_B^2}{kT} \mathbf{g} \cdot \langle \mathbf{SS} \rangle \cdot \mathbf{g}^T \quad (1.25)$$

In the linear regime, the proportionality constant relating the induced electron magnetic moment and the magnetic field is thus dictated by the magnetic susceptibility per molecule $\boldsymbol{\chi}$ according to the following equation:

$$\langle \boldsymbol{\mu}_\mathbf{S} \rangle = \frac{\boldsymbol{\chi} \cdot \mathbf{B_0}}{\mu_0} \quad (1.26)$$

The tensor $\boldsymbol{\chi}$ takes into account both the anisotropy of $\mathbf{g}$ and the anisotropy of $\mathbf{S_C}$ due to ZFS or coupling of the ground state with excited states, and it is thus an anisotropic quantity. The principal values of

$\boldsymbol{\chi}$ (χ_{xx}, χ_{yy}, χ_{zz}) are labelled in order to have the χ_{zz} component as the most separated of the three components, so that the anisotropy parameters

$$\Delta\chi_{ax} = \chi_{zz} - \frac{\chi_{xx} + \chi_{yy}}{2} \qquad (1.27)$$

$$\Delta\chi_{rh} = \chi_{xx} - \chi_{yy}$$

obey the relationship $|\Delta\chi_{rh}| \leq 2|\Delta\chi_{ax}|/3$.

The energy related to the (thermal average) induced electron magnetic moment (see eqn (1.12)) is thus

$$E = -\int \langle \boldsymbol{\mu}_{\mathbf{S}} \rangle \cdot \mathrm{d}\mathbf{B_0} = -\frac{\mu_B^2}{kT} \frac{\mathbf{B_0} \cdot \mathbf{g} \cdot \langle \mathbf{SS} \rangle \cdot \mathbf{g}^T \cdot \mathbf{B_0}}{2} = -\frac{\mathbf{B_0} \cdot \boldsymbol{\chi} \cdot \mathbf{B_0}}{2\mu_0} \qquad (1.28)$$

and therefore it depends on the orientation of $\mathbf{B_0}$ with respect to the molecule.

In the case of $S = 1$ and axial ZFS (see eqn (1.23)),

$$\boldsymbol{\chi} = \frac{\mu_0 \mu_B^2}{kT} \times$$

$$\begin{pmatrix} g_{xx}^2 \dfrac{2kT}{D} \dfrac{1 - \exp\left(-\dfrac{D}{kT}\right)}{2\exp\left(-\dfrac{D}{kT}\right) + 1} & 0 & 0 \\ 0 & g_{yy}^2 \dfrac{2kT}{D} \dfrac{1 - \exp\left(-\dfrac{D}{kT}\right)}{2\exp\left(-\dfrac{D}{kT}\right) + 1} & 0 \\ 0 & 0 & g_{zz}^2 \dfrac{2\exp\left(-\dfrac{D}{kT}\right)}{2\exp\left(-\dfrac{D}{kT}\right) + 1} \end{pmatrix} \qquad (1.29)$$

Analogous equations can be calculated for other spin multiplicities.[3]

1.2 The Hyperfine Shift

The hyperfine shift is the difference in the resonance frequency of a nuclear transition between states differing by $\Delta m_I = \pm 1$ in the absence of the paramagnetic center and in its presence, scaled by the nuclear Larmor frequency ($\gamma_I B_0/2\pi$). It is thus related to the energy of the hyperfine coupling (eqn (1.4)) between nuclear and electron magnetic moments.

Electrons change their spin state much faster than protons, due to their more efficient relaxation pathways. As a consequence, the nucleus sees the unpaired electron(s) changing its state rapidly among the possible m_S levels before being able to change its own m_I energy level. This implies that the nuclear magnetic moment actually interacts with the electron induced magnetic moment, calculated from the average of their population distribution at the temperature of the system (see previous section). Therefore, using eqn (1.4) and (1.22), the hyperfine shift is

$$\delta^{\mathrm{hs}} = -\frac{\mathbf{S_C}\cdot\mathbf{A}\cdot\mathbf{I}}{\hbar\gamma_I B_0 m_I} = \frac{\mu_{\mathrm{B}}}{\hbar\gamma_I kT}\boldsymbol{\iota}\cdot\mathbf{g}\cdot\langle\mathbf{SS}\rangle\cdot\mathbf{A}\cdot\boldsymbol{\iota} \tag{1.30}$$

where $\boldsymbol{\iota}$ indicates the magnetic field direction. It is convenient to define a hyperfine shielding tensor $\boldsymbol{\sigma}^{\mathbf{hs}}$:[4]

$$\boldsymbol{\sigma}^{\mathbf{hs}} = -\frac{\mu_{\mathrm{B}}}{\hbar\gamma_I kT}\mathbf{g}\cdot\langle\mathbf{SS}\rangle\cdot\mathbf{A} \tag{1.31}$$

from which the shifts can be easily calculated for the different directions of the magnetic field. In the case of isotropic molecular reorientation, *i.e.* of isotropically oriented magnetic fields, the hyperfine shift (called in this case the isotropic hyperfine shift) becomes

$$\delta^{\mathrm{hs}} = -\frac{\mathrm{Tr}(\boldsymbol{\sigma}^{\mathbf{hs}})}{3} = \delta^{\mathrm{cs}} + \delta^{\mathrm{pcs}} \tag{1.32}$$

where Tr indicates the trace, *i.e.* the sum of the diagonal terms, of the $\boldsymbol{\sigma}^{\mathbf{hs}}$ matrix.[5] In writing eqn (1.32) it was also assumed that the magnetic field direction changes on a time scale slower than the electron relaxation time, *i.e.* that the molecular reorientation time is longer than the electron relaxation time.

In the quantum chemistry formalism, the shielding tensor is defined as the second partial derivative of the thermally averaged energy with respect to the magnetic field and to the nuclear magnetic moment, calculated at zero magnetic field and zero magnetic moment:[6,7]

$$\boldsymbol{\sigma} = \left.\frac{\partial^2\langle E\rangle}{\partial\mathbf{B_0}\partial\boldsymbol{\mu}_\mathbf{I}}\right|_{B_0=\mu_I=0} \tag{1.33}$$

From eqn (1.5), it is found that[8–10]

$$\boldsymbol{\sigma}^{\mathbf{hs}} = -\frac{1}{kT}\times \frac{\sum_{mn} Q_{mn}\langle n|\left.\frac{\partial(\mu_{\mathrm{B}}\mathbf{B_0}\cdot\mathbf{g}\cdot\mathbf{S}+H_{\mathrm{hc}})}{\partial\mathbf{B_0}}\right|_{B_0=\mu_I=0}|m\rangle\langle m|\left.\frac{\partial(\mu_{\mathrm{B}}\mathbf{B_0}\cdot\mathbf{g}\cdot\mathbf{S}+H_{\mathrm{hc}})}{\partial\boldsymbol{\mu}_\mathbf{I}}\right|_{B_0=\mu_I=0}|n\rangle}{\sum_n \exp\left[-E_n^0/(kT)\right]}$$

$$= -\frac{\mu_{\mathrm{B}}}{\hbar\gamma_I kT}\mathbf{g}\cdot\langle\mathbf{SS}\rangle\cdot\mathbf{A} \tag{1.34}$$

As already anticipated in Section 1.1, the operator **A** is split in the Fermi-contact (A^{FC}) and dipolar ($\mathbf{A}^{DIP}$) components, which in solution provide the contact (δ^{cs}) and pseudocontact (δ^{pcs}) shifts, respectively.

1.2.1 The Fermi-contact Shift

The contact shift arises from the delocalization of the unpaired electron spin(s), in particular at the site of the detected nucleus. It is thus proportional to the unpaired electron spin density, ρ, present at the nucleus (i) through direct overlap between the molecular orbital(s) containing the unpaired electron(s) and the s orbitals (allowing for a non-zero electron density at the nucleus) of the observed nucleus, and (ii) due to spin polarization of paired electrons. When an unpaired electron in a d orbital of a metal is partially delocalized to an overlapping p or d orbital of a covalently bound atom, in fact, the spin polarization mechanism induces unpaired electron spin density at the nucleus of this atom because, among the paired electrons in an s orbital, the electron with spin parallel to the unpaired electron spin has a slight preference to occupy the region of space closer to that of the unpaired electron (Hund's rule). In this way the electron with spin antiparallel to the unpaired electron has a larger spin density on the nucleus, and the difference in the spin densities corresponding to the two states provides the unpaired spin density. In the presence of direct molecular overlap with an s orbital, the spin density at the nucleus is positive, whereas in the case of spin polarization, it is negative.

As is clear from eqn (1.6), (1.7), (1.31), (1.32) and (1.34), in isotropic systems the contact shift is given by[3,11]

$$\delta^{cs} = -\frac{\mathrm{Tr}(\boldsymbol{\sigma}^{FC})}{3} \tag{1.35}$$

where

$$\begin{aligned}\boldsymbol{\sigma}^{FC} &= -\frac{\mu_B}{\hbar\gamma_I kT}\mathbf{g}\cdot\langle\mathbf{SS}\rangle\cdot\mathbf{A}^{FC} = -\frac{\mu_B A^{FC}}{\hbar\gamma_I kT}\mathbf{g}\cdot\langle\mathbf{SS}\rangle\cdot\mathbf{1}\\ &= -\frac{\mu_0\mu_B^2 g_e\rho}{3SkT}\mathbf{g}\cdot\langle\mathbf{SS}\rangle\cdot\mathbf{1}\end{aligned} \tag{1.36}$$

The last expression in eqn (1.36) clarifies that the contact shifts do not depend on the nuclear parameters; they depend on the electronic parameters and on the unpaired spin(s) density at the nucleus.

When **g** is orientation dependent, in isotropic systems

$$\delta^{cs} = \frac{A^{FC}}{\hbar}\frac{g_{xx}+g_{yy}+g_{zz}}{3}\frac{\mu_B S(S+1)}{3\gamma_I kT} \tag{1.37}$$

In $S=1$ systems with axial ZFS (see eqn (1.23)),

$$\delta^{\mathrm{cs}} = \frac{A^{\mathrm{FC}}}{\hbar}\frac{\mu_{\mathrm{B}}}{\gamma_I kT}\frac{\mathrm{Tr}(\mathbf{g}\cdot\langle\mathbf{SS}\rangle\cdot\mathbf{1})}{3} = \frac{A^{\mathrm{FC}}}{\hbar}\frac{\mu_{\mathrm{B}}}{3\gamma_I kT}$$
$$\times \mathrm{Tr}\begin{pmatrix} \frac{2g_{xx}kT}{D}\frac{1-\exp\left(-\frac{D}{kT}\right)}{2\exp\left(-\frac{D}{kT}\right)+1} & 0 & 0 \\ 0 & \frac{2g_{yy}kT}{D}\frac{1-\exp\left(-\frac{D}{kT}\right)}{2\exp\left(-\frac{D}{kT}\right)+1} & 0 \\ 0 & 0 & \frac{2g_{zz}\exp\left(-\frac{D}{kT}\right)}{2\exp\left(-\frac{D}{kT}\right)+1} \end{pmatrix} \tag{1.38}$$

which, to the first order in $D/(kT)$, is equal to[3]

$$\delta^{\mathrm{cs}} = \frac{A^{\mathrm{FC}}}{\hbar}\frac{2\mu_{\mathrm{B}}}{3\gamma_I kT}\mathrm{Tr}\begin{pmatrix} \frac{g_{xx}}{3}\left(1+\frac{1}{6}\frac{D}{kT}\right) & 0 & 0 \\ 0 & \frac{g_{yy}}{3}\left(1+\frac{1}{6}\frac{D}{kT}\right) & 0 \\ 0 & 0 & \frac{g_{zz}}{3}\left(1-\frac{1}{3}\frac{D}{kT}\right) \end{pmatrix}$$
$$= \frac{A^{\mathrm{FC}}}{\hbar}\frac{2\mu_{\mathrm{B}}}{3\gamma_I kT}\frac{g_{xx}+g_{yy}+g_{zz}}{3}\left(1+\frac{g_{xx}+g_{yy}-2g_{zz}}{6(g_{xx}+g_{yy}+g_{zz})}\frac{D}{kT}\right) \tag{1.39}$$

This results in a temperature dependence which is not linear in T^{-1}, but has also a T^{-2} contribution. The presence of such a (usually minor) contribution can be detected in a temperature dependence plot by noting that, assuming a linear dependence, the contact shift does not extrapolate to zero for $T^{-1}=0$. Analogous equations can be calculated for other spin multiplicities.[3]

Only nuclei experiencing a non-zero unpaired electron spin density experience contact shifts. This implies that contact shifts are present only

for atoms within a few bonds from the paramagnetic center. The magnitude of the shift depends, of course, on the A^{FC} constant, which in turn depends on the geometrical arrangement of the overlapping orbitals. Equations of the Karplus type have been introduced to describe the contact shifts as a function of dihedral angles θ defined according to the binding directions,

$$\delta^{cs} = a\ \cos^2\ \theta + b\ \cos\ \theta + c \tag{1.40}$$

or

$$\delta^{cs} = a\ \sin^2\ \theta + b\ \cos\ \theta + c \tag{1.41}$$

(depending on the relative orientation of the involved orbitals), where a, b, and c are constants.[12–14]

Euristic Karplus-type equations were also obtained for hyperfine shifts (comprising both the contact and the pseudocontact contributions) of methyl protons in low spin iron(III) heme proteins with one or two histidines as axial ligands,[15] and in high spin iron(II) heme proteins.[16] In these proteins, the methyl proton hyperfine shifts depend on the angle(s) formed by the axial histidine plane(s) and the planar ligands.

1.2.2 The Pseudocontact Shift

The pseudocontact shift (PCS) results from the dipole–dipole interaction between the nucleus and the electron magnetic moment occurring through space, and thus not requiring molecular binding. For an accurate evaluation of this NMR observable, the distribution of the electron spin over the space should be considered. However, to simplify the problem, the electron spin is commonly considered located at a single point (*i.e.*, the metal nucleus in a paramagnetic metal ion) in the so-called metal centered point-dipole approximation (Section 1.2.2.1). We will then see how the problem can be faced outside this approximation (Section 1.2.2.2).

1.2.2.1 The Point-dipole Approximation

As is clear from eqn (1.6), (1.9), (1.31), (1.32) and (1.34), in isotropic systems the PCS is given by

$$\delta^{pcs} = -\frac{\mathrm{Tr}(\boldsymbol{\sigma}^{DIP})}{3} \tag{1.42}$$

where

$$\boldsymbol{\sigma}^{DIP} = -\frac{\mu_B}{\hbar\gamma_I kT}\mathbf{g}\cdot\langle\mathbf{SS}\rangle\cdot\mathbf{A}^{DIP} = -\frac{\mu_B}{\hbar\gamma_I kT}\mathbf{g}\cdot\langle\mathbf{SS}\rangle\cdot\frac{\mu_0}{4\pi}\frac{\hbar\gamma_I\mu_B}{r^3}\mathbf{g}^T\cdot\left(\frac{3\mathbf{rr}}{r^2}-\mathbf{1}\right) \tag{1.43}$$

and thus, using eqn (1.25),

$$\boldsymbol{\sigma}^{\mathrm{DIP}} = -\frac{1}{4\pi r^3}\boldsymbol{\chi}\cdot\left(\frac{3\mathbf{rr}}{r^2}-\mathbf{1}\right) \tag{1.44}$$

Therefore, in the absence of preferential orientations of the molecule with respect to the magnetic field

$$\delta^{\mathrm{pcs}} = \frac{1}{12\pi r^5}\mathrm{Tr}\left[\begin{pmatrix}\chi_{xx} & \chi_{xy} & \chi_{xz}\\ \chi_{xy} & \chi_{yy} & \chi_{yz}\\ \chi_{xz} & \chi_{yz} & \chi_{zz}\end{pmatrix}\begin{pmatrix}3x^2-r^2 & 3xy & 3xz\\ 3xy & 3y^2-r^2 & 3yz\\ 3xz & 3yz & 3z^2-r^2\end{pmatrix}\right] \tag{1.45}$$

which can be rewritten as

$$\delta^{\mathrm{pcs}} = \frac{1}{12\pi r^5}\times \left[\chi_{xx}(3x^2-r^2)+\chi_{yy}(3y^2-r^2)+\chi_{zz}(3z^2-r^2)+6\chi_{xy}xy+6\chi_{xz}xz+6\chi_{yz}yz\right] \tag{1.46}$$

or, using the spherical coordinates r, θ and ϕ (see Figure 1.2(a)) to identify the position of a nucleus, with the electron assumed in the origin of the reference frame,

$$\delta^{\mathrm{pcs}} = \frac{1}{4\pi r^3}\left[(\chi_{zz}-\chi_{\mathrm{iso}})\frac{3\cos^2\theta-1}{2}+(\chi_{xx}-\chi_{yy})\frac{\sin^2\theta\cos 2\phi}{2} + \chi_{xy}\sin^2\theta\sin 2\phi+\chi_{xz}\sin 2\theta\cos\phi+\chi_{yz}\sin 2\theta\sin\phi\right] \tag{1.47}$$

where

$$\chi_{\mathrm{iso}} = \frac{\mathrm{Tr}(\boldsymbol{\chi})}{3} \tag{1.48}$$

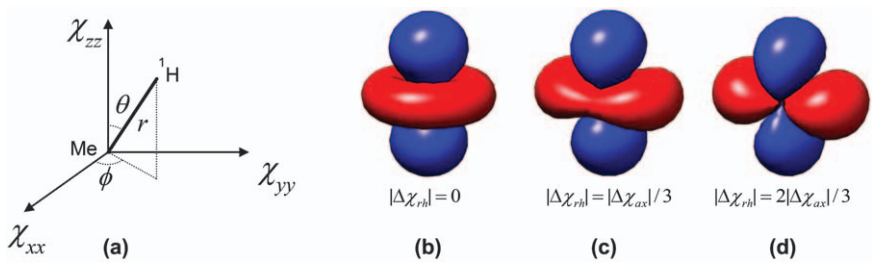

Figure 1.2 (a) Spherical coordinates defining the position of the nucleus in the frame of the $\boldsymbol{\chi}$ tensor and (b)–(d) surfaces with constant absolute PCS value (blue = positive, red = negative) for different rhombicities of the $\boldsymbol{\chi}$ tensor.

Eqn (1.47) can also be written as[17]

$$\delta^{\mathrm{pcs}} = \frac{1}{4\pi r^3} \sum_{q=-2}^{2} \zeta_q Y_2^q \tag{1.49}$$

where

$$\zeta_0 = 2\sqrt{\frac{\pi}{5}}(\chi_{zz} - \chi_{\mathrm{iso}}) = 4\sqrt{\frac{\pi}{45}}\Delta\chi_{ax}$$

$$\zeta_{\pm 1} = \mp 2\sqrt{\frac{2\pi}{15}}\left(\chi_{xz} \mp i\chi_{yz}\right)$$

$$\zeta_{\pm 2} = \sqrt{\frac{2\pi}{15}}\left[\left(\chi_{xx} - \chi_{yy}\right) \mp 2i\chi_{xy}\right]$$

and Y_2^q are the second order spherical harmonics

$$Y_2^0 = \frac{1}{4}\sqrt{\frac{5}{\pi}}\left(3\cos^2\theta - 1\right),\ Y_2^{\pm 1} = \mp\frac{1}{2}\sqrt{\frac{15}{2\pi}}\sin\theta\cos\theta\exp(\pm i\phi),$$

$$Y_2^{\pm 2} = \frac{1}{4}\sqrt{\frac{15}{2\pi}}\sin^2\theta\exp(\pm 2i\phi)$$

In the case where the axes of the reference frame are chosen to coincide with the main directions of the $\boldsymbol{\chi}$ tensor (*i.e.*, χ_{xy}, χ_{xz} and χ_{yz} in eqn (1.46) are all equal to zero), eqn (1.47) simplifies to

$$\delta^{\mathrm{pcs}} = \frac{1}{12\pi r^3}\left[\Delta\chi_{ax}(3\cos^2\theta - 1) + \frac{3}{2}\Delta\chi_{rh}\sin^2\theta\cos 2\phi\right] \tag{1.50}$$

where $\Delta\chi_{ax}$ and $\Delta\chi_{rh}$ are defined as in eqn (1.27). Of note, the PCSs do not depend on the magnitude of the magnetic susceptibility tensor but only on its anisotropy, *i.e.*, for an isotropic $\boldsymbol{\chi}$, $\delta^{\mathrm{pcs}} = 0$. They are also independent of the nuclear parameters, being the same for, *e.g.*, ^{1}H, ^{13}C or ^{15}N nuclei, if placed in the same position. Figure 1.2(b) shows the surfaces with constant PCS value for different choices of $\Delta\chi_{rh}/\Delta\chi_{ax}$. The dependence of PCSs on the nuclear coordinates expressed in a common frame makes these NMR observables useful for molecular structural characterization (see Sections 3.3 and 4.2).[18–32]

If α, β and γ are the Euler angles describing the rotation from any molecular frame to the frame with axes coinciding with the main directions of

the $\boldsymbol{\chi}$ tensor, the anisotropic part of the $\boldsymbol{\chi}$ tensor in the molecular frame is given by

$$\boldsymbol{\chi} - \chi_{\mathrm{iso}}\mathbf{1} = \mathbf{R}(\alpha,\beta,\gamma)^T \begin{pmatrix} -\frac{\Delta\chi_{ax}}{3} + \frac{\Delta\chi_{rh}}{2} & 0 & 0 \\ 0 & -\frac{\Delta\chi_{ax}}{3} - \frac{\Delta\chi_{rh}}{2} & 0 \\ 0 & 0 & \frac{2}{3}\Delta\chi_{ax} \end{pmatrix} \mathbf{R}(\alpha,\beta,\gamma) \tag{1.51}$$

where $\mathbf{R}$ is the rotation matrix allowing for the change of the reference frame.[33] In summary, the PCSs can be calculated from the nuclear coordinates of the paramagnetic molecule and (i) the five components of the anisotropic part of the symmetric $\boldsymbol{\chi}$ tensor (eqn (1.47)) or (ii) the two anisotropic parameters $\Delta\chi_{ax}$ and $\Delta\chi_{rh}$ and the three Euler angles describing the orientation of the main axes of the $\boldsymbol{\chi}$ tensor (eqn (1.50) and (1.51)).

For an $S = 1$ system with axial ZFS (from eqn (1.50) and (1.29)), to the first order in $D/(kT)$,

$$\delta^{\mathrm{pcs}} = \frac{\mu_0}{4\pi}\frac{\mu_B^2}{9kT}\left[\left(2g_{zz}^2 - g_{xx}^2 - g_{yy}^2\right)\frac{3\cos^2\theta - 1}{r^3}\left(1 - \frac{1}{6}\frac{4g_{zz}^2 + g_{xx}^2 + g_{yy}^2}{2g_{zz}^2 - g_{xx}^2 - g_{yy}^2}\frac{D}{kT}\right)\right.$$
$$\left. + \left(g_{xx}^2 - g_{yy}^2\right)\frac{\sin^2\theta\cos 2\phi}{r^3}\left(1 + \frac{1}{6}\frac{D}{kT}\right)\right] \tag{1.52}$$

Different to contact shifts (eqn (1.39)), for PCSs the term in T^{-2} is usually larger than the term in T^{-1}. Analogous equations can be calculated for other spin multiplicities.[3]

1.2.2.2 *Breaking the Point-dipole Approximation*

Unpaired electrons are certainly not localized on a single atom but spread over the ligand atoms through molecular overlap. The resulting effect is that the dipole–dipole interaction between the nucleus and all fractions of the distributed electron magnetic moment should be considered. In a semiclassical approach, this has been done by calculating the sum of point-dipole contributions arising from the fractional magnetic moments located in corresponding positions with high electron density.[34] Of course, the further the nucleus is from the paramagnetic center, the smaller the error in neglecting such an electron distribution: the dipolar interaction for nuclei far from the paramagnetic center is well approximated by considering the unpaired electron at a single point. It was shown, for instance, that in a high spin cobalt(II) system, the point-dipole approximation provides well predicted shifts for nuclei at distances further than 8 Å from the metal.[35]

Recently, it has been shown that the hyperfine shifts outside the point-dipole approximation can be calculated by integration over space of eqn (1.44) after multiplication of the electron density function $\rho(\mathbf{r_e})$:[17]

$$\boldsymbol{\sigma}^{\mathbf{DIP}} = \frac{1}{4\pi}\int\left(\frac{3(\mathbf{r_e}-\mathbf{r})(\mathbf{r_e}-\mathbf{r})}{|\mathbf{r_e}-\mathbf{r}|^5} - \frac{\mathbf{1}}{|\mathbf{r_e}-\mathbf{r}|^3}\right)\cdot\boldsymbol{\chi}(\mathbf{r_e})\rho(\mathbf{r_e})\mathrm{d}^3\mathbf{r_e} \tag{1.53}$$

This corresponds to calculating the convolution

$$\boldsymbol{\sigma}^{\mathbf{DIP}} = \frac{1}{4\pi}\left[\frac{3\mathbf{rr}}{r^5} - \frac{\mathbf{1}}{r^3}\right]*[\boldsymbol{\chi}(\mathbf{r})\rho(\mathbf{r})] \tag{1.54}$$

which can be done using the Fourier transform and the differential operators (corresponding to vectors in the reciprocal space). Numerical solutions of the inverse problem can provide the electron density function (under some regularization conditions, due to the ill-posed nature of the problem) from the pseudoconctact shifts and the atomic coordinates.[17,36]

1.2.3 Simplified Expressions in Limiting Cases

In the absence of low-lying electronically excited states, the thermally accessible electronic states are limited to the eigenstates of the ZFS, and when ZFS is absent $\langle\mathbf{SS}\rangle = \frac{S(S+1)}{3}\mathbf{1}$ (and thus $\mathrm{Tr}(\langle\mathbf{SS}\rangle) = S(S+1)$). Therefore, in the limit of no ZFS and no interactions of the ground S multiplet with the excited states (second order Zeeman mixing), eqn (1.20) indicates that the three values of $\langle\mu_S\rangle$for the three main directions of the **g**-frame are

$$\langle\mu_S\rangle_k = \frac{g_{kk}^2\mu_\mathrm{B}^2 B_0 S(S+1)}{3kT} \tag{1.55}$$

and, if there are also no orbital contributions ($\mathbf{g} = g_\mathrm{e}\mathbf{1}$), from eqn (1.10) and (1.22),

$$\langle S_z\rangle = -\frac{g_\mathrm{e}\mu_\mathrm{B}B_0 S(S+1)}{3kT} \tag{1.56}$$

In this simple case, $\mathbf{S_C}$ is directed along $\mathbf{B_0}$.

Only in the case of no ZFS, of a singly populated S manifold, and of the validity of eqn (1.55) (electron Zeeman energy is much smaller than thermal energy, excited states are not coupled to the ground state, $\langle\mathbf{SS}\rangle = \frac{S(S+1)}{3}\mathbf{1}$), the principal axes of $\boldsymbol{\chi}$ and **g** coincide, and eqn (1.25) provides

$$\chi_{kk} = \frac{\mu_0\mu_\mathrm{B}^2 g_{kk}^2 S(S+1)}{3kT}, \tag{1.57}$$

and if **g** is also isotropic ($\mathbf{g} = g_\mathrm{e}\mathbf{1}$), the magnetic susceptibility becomes isotropic and equal to

$$\chi = \frac{\mu_0\mu_\mathrm{B}^2 g_\mathrm{e}^2 S(S+1)}{3kT} \tag{1.58}$$

which is known as Curie law. In these conditions, $\boldsymbol{\sigma}^{\mathbf{FC}}$ is also isotropic and the contact shift (eqn (1.35) and (1.36)) is given by[37]

$$\delta^{\mathrm{cs}} = \frac{A^{\mathrm{FC}}}{\hbar}\frac{g_e\mu_B S(S+1)}{3\gamma_I kT} \tag{1.59}$$

whereas the PCS is zero. On the other hand, in the case of the validity of eqn (1.57), from eqn (1.50),

$$\delta^{\mathrm{pcs}} = \frac{\mu_0}{4\pi}\frac{\mu_B^2 S(S+1)}{18kTr^3}\left[(2g_{zz}^2 - g_{xx}^2 - g_{yy}^2)(3\cos^2\theta - 1) + 3(g_{xx}^2 - g_{yy}^2)\sin^2\theta\cos 2\phi\right] \tag{1.60}$$

1.2.4 The Effect of Partial Self-orientation

The presence of anisotropy in the magnetic susceptibility tensor makes the energy of the different orientations of a molecule in a magnetic field also anisotropic. In fact, the energy related to the induced electron magnetic moment depends on the orientation of $\langle\boldsymbol{\mu}_{\mathbf{S}}\rangle$ with respect to $\mathbf{B_0}$, and thus, it is different depending on the magnetic field direction, as described by eqn (1.28). Therefore, the molecule does not have the same probability to sample each orientation, and a partial alignment occurs. The degree of alignment can be described by a probability tensor **P**. The latter indicates the probabilities that the magnetic field forms the angles α_i with the main directions i of the $\boldsymbol{\chi}$ tensor. Therefore, using eqn (1.28), along the principal components of the $\boldsymbol{\chi}$ tensor

$$P_{xx} = \frac{\int_\Omega \cos^2\alpha_x \exp\left(-\frac{E_x}{kT}\right)\sin\alpha_x \mathrm{d}\alpha_x \mathrm{d}\beta_x}{\int_\Omega \exp\left(-\frac{E_x}{kT}\right)\sin\alpha_x \mathrm{d}\alpha_x \mathrm{d}\beta_x}$$

$$= \frac{\int\cos^2\alpha_x \ \exp\left[\frac{B_0^2}{2\mu_0 kT}(\chi_{xx}\cos^2\alpha_x + \chi_{yy}\sin^2\alpha_x\cos^2\beta_x + \chi_{zz}\sin^2\alpha_x\sin^2\beta_x)\right]\mathrm{d}\cos\alpha_x\mathrm{d}\beta_x}{\int\exp\left[\frac{B_0^2}{2\mu_0 kT}(\chi_{xx}\cos^2\alpha_x + \chi_{yy}\sin^2\alpha_x\cos^2\beta_x + \chi_{zz}\sin^2\alpha_x\sin^2\beta_x)\right]\mathrm{d}\cos\alpha_x\mathrm{d}\beta_x}$$

$$P_{yy} = \frac{\int\cos^2\alpha_y \ \exp\left[\frac{B_0^2}{2\mu_0 kT}(\chi_{yy}\cos^2\alpha_y + \chi_{xx}\sin^2\alpha_y\cos^2\beta_y + \chi_{zz}\sin^2\alpha_y\sin^2\beta_y)\right]\mathrm{d}\cos\alpha_y\mathrm{d}\beta_y}{\int\exp\left[\frac{B_0^2}{2\mu_0 kT}(\chi_{yy}\cos^2\alpha_y + \chi_{xx}\sin^2\alpha_y\cos^2\beta_y + \chi_{zz}\sin^2\alpha_y\sin^2\beta_y)\right]\mathrm{d}\cos\alpha_y\mathrm{d}\beta_y}$$

$$P_{zz} = \frac{\int\cos^2\alpha_z \ \exp\left[\frac{B_0^2}{2\mu_0 kT}(\chi_{zz}\cos^2\alpha_z + \chi_{xx}\sin^2\alpha_z\cos^2\beta_z + \chi_{yy}\sin^2\alpha_z\sin^2\beta_z)\right]\mathrm{d}\cos\alpha_z\mathrm{d}\beta_z}{\int\exp\left[\frac{B_0^2}{2\mu_0 kT}(\chi_{zz}\cos^2\alpha_z + \chi_{xx}\sin^2\alpha_z\cos^2\beta_z + \chi_{yy}\sin^2\alpha_z\sin^2\beta_z)\right]\mathrm{d}\cos\alpha_z\mathrm{d}\beta_z} \tag{1.61}$$

where α_x and β_x, α_y and β_y, and α_z and β_z are the spherical angles describing the orientation of the magnetic field with respect to the x, y and z main axes

of the χ tensor, respectively. The results of the integrals at the first order in E_i/kT are

$$\begin{aligned} P_{xx} &= \frac{1}{3}\left(1+\frac{2}{15}\frac{B_0^2}{\mu_0 kT}\left(\chi_{xx}-\frac{\chi_{yy}+\chi_{zz}}{2}\right)\right) \\ P_{yy} &= \frac{1}{3}\left(1+\frac{2}{15}\frac{B_0^2}{\mu_0 kT}\left(\chi_{yy}-\frac{\chi_{xx}+\chi_{zz}}{2}\right)\right) \\ P_{zz} &= \frac{1}{3}\left(1+\frac{2}{15}\frac{B_0^2}{\mu_0 kT}\left(\chi_{zz}-\frac{\chi_{xx}+\chi_{yy}}{2}\right)\right) \end{aligned} \tag{1.62}$$

i.e.,

$$P_{ii} = \frac{1}{3}\left(1+\frac{B_0^2}{5\mu_0 kT}\left(\chi_{ii}-\chi_{\mathrm{iso}}\right)\right) \tag{1.63}$$

As expected, $P_{xx}+P_{yy}+P_{zz}=1$. In eqn (1.61)–(1.63) the magnetic susceptibility to be considered is the overall magnetic susceptibility tensor, composed of the paramagnetic and the diamagnetic contributions. In fact, the interaction of the magnetic field with the motions of paired electrons in their orbitals may produce an anisotropic magnetic moment, due to the possible anisotropy of the electron current, which causes an anisotropic $\boldsymbol{\chi}^{\mathbf{dia}}$. Therefore, the χ-tensor components contained in the $\boldsymbol{\sigma}$ tensor are not equal to those contained in the **P** tensor, although for simplicity they are indicated here with the same symbols. The diamagnetic susceptibility is roughly proportional to the molecular weight, and thus $\boldsymbol{\chi}^{\mathbf{dia}}$ might not be negligible in macromolecules or when multiple aromatic planes are stacked together, as in nucleic acids or bicelles.

The hyperfine shifts average to values which depend on the components of the shielding tensor $\boldsymbol{\sigma}$ along the main directions of the probability tensor **P**. Therefore, the PCSs are (see eqn (1.44))

$$\begin{aligned} \delta^{\mathrm{pcs}} = -\left(\sigma_{xx}^{\mathrm{DIP}}P_{xx}+\sigma_{yy}^{\mathrm{DIP}}P_{yy}+\sigma_{zz}^{\mathrm{DIP}}P_{zz}\right) = \frac{1}{4\pi r^5} \\ \times\mathrm{Tr}\left[\begin{pmatrix}\chi_{xx}&0&0\\0&\chi_{yy}&0\\0&0&\chi_{zz}\end{pmatrix}\begin{pmatrix}3x^2-r^2&3xy&3xz\\3xy&3y^2-r^2&3yz\\3xz&3yz&3z^2-r^2\end{pmatrix}\begin{pmatrix}P_{xx}&0&0\\0&P_{yy}&0\\0&0&P_{zz}\end{pmatrix}\right] \end{aligned} \tag{1.64}$$

and thus, in spherical coordinates,

$$\begin{aligned} \delta^{\mathrm{pcs}} = \frac{1}{12\pi r^3}\left\{\Delta\chi_{ax}\left(3\cos^2\theta-1\right)\left[1+\frac{B_0^2}{15\mu_0 kT}\left(\left(2\chi_{zz}+\frac{\chi_{xx}+\chi_{yy}}{2}\right)-\frac{3}{4}\frac{\Delta\chi_{rh}^2}{\Delta\chi_{ax}}\right)\right]\right. \\ \left.+\frac{3}{2}\Delta\chi_{rh}\sin^2\theta\cos 2\varphi\left(1+\frac{B_0^2}{15\mu_0 kT}\left(2\chi_{xx}+2\chi_{yy}-\chi_{zz}\right)\right)\right\} \end{aligned} \tag{1.65}$$

where θ is the angle between the metal–nucleus vector $\mathbf{r}$ and the z axis of the diagonal $\boldsymbol{\chi}$ tensor, and φ is an angle related to the projection of $\mathbf{r}$ on the xy plane of the tensor.

This correction to the PCS value is in most cases minor, and thus usually neglected. At very high fields (>20 T), when it may become important, the paramagnetic susceptibility becomes field dependent, as described by the Brillouin equation, and this affects the PCSs as much as the self-orientation effect.[38] An analogous correction should also be applied to the contact shift, but again it is usually not taken into account because it is considered smaller than the error of the experimental data.

NMR shifts in paramagnetic molecules can also be affected by the residual anisotropic chemical shifts (RACS), which arise in the presence of partial alignment, and thus also of the self-alignment caused by the anisotropy of the $\boldsymbol{\chi}$ tensor. These contributions to the shift originate from the anisotropy of the chemical shift (CSA) tensor, and should thus be evaluated for an accurate calculation of the PCSs, when the latter are obtained from the difference of the NMR shifts between the paramagnetic molecule and a diamagnetic analogue.[39,40]

1.3 The Paramagnetic Residual Dipolar Couplings

Partial alignment of a molecule causes the occurrence of residual dipolar couplings (RDCs). RDCs in fact result from the non-zero average of the dipole–dipole interaction energy between nuclear magnetic moments, occurring when not all molecular orientations have the same probability. Since the dipolar energy is equal to

$$E^{\mathrm{dip}} = \mathbf{I_1} \cdot \mathbf{a^{DIP}} \cdot \mathbf{I_2} = \frac{\mu_0}{4\pi} \frac{\hbar^2 \gamma_{I_1} \gamma_{I_2}}{r_{12}^3} \left(\frac{3\mathbf{r_{12}}\mathbf{r_{12}}}{r_{12}^2} - \mathbf{1} \right) \tag{1.66}$$

where $\mathbf{r_{12}}$ is the vector connecting the coupled nuclei $\mathbf{I_1}$ and $\mathbf{I_2}$, with magnetic moments oriented along the direction of $\mathbf{B_0}$, the RDCs are given by

$$\Delta\nu^{\mathrm{rdc}} = \frac{\langle E^{\mathrm{dip}} \rangle}{h} = -\frac{\mu_0 \hbar \gamma_{I_1} \gamma_{I_2}}{8\pi^2 r_{12}^5} \times \mathrm{Tr} \left[\begin{pmatrix} 3x^2 - r^2 & 3xy & 3xz \\ 3xy & 3y^2 - r^2 & 3yz \\ 3xz & 3yz & 3z^2 - r^2 \end{pmatrix} \begin{pmatrix} P_{xx} & 0 & 0 \\ 0 & P_{yy} & 0 \\ 0 & 0 & P_{zz} \end{pmatrix} \right] \tag{1.67}$$

Therefore, paramagnetic RDCs (pRDCs) are described, in the main frame of the χ tensor, by

$$\Delta\nu^{\mathrm{rdc}} = -\frac{\mu_0\hbar\gamma_{I_1}\gamma_{I_2}}{8\pi^2 r_{12}^5}\mathrm{Tr}\left[\begin{pmatrix} 3x^2-r^2 & 3xy & 3xz \\ 3xy & 3y^2-r^2 & 3yz \\ 3xz & 3yz & 3z^2-r^2 \end{pmatrix}\times \right.$$
$$\left.\begin{pmatrix} \frac{1}{3}\left(1+\frac{B_0^2}{5\mu_0 kT}\left(\chi_{xx}-\chi_{\mathrm{iso}}\right)\right) & 0 & 0 \\ 0 & \frac{1}{3}\left(1+\frac{B_0^2}{5\mu_0 kT}\left(\chi_{yy}-\chi_{\mathrm{iso}}\right)\right) & 0 \\ 0 & 0 & \frac{1}{3}\left(1+\frac{B_0^2}{5\mu_0 kT}\left(\chi_{zz}-\chi_{\mathrm{iso}}\right)\right) \end{pmatrix}\right] \quad (1.68)$$

which, since $\Delta\nu^{\mathrm{rdc}} = 0$ if $P_{ii} = \frac{1}{3}$, can be written as

$$\Delta\nu^{\mathrm{rdc}} = -\frac{\mu_0\hbar\gamma_{I_1}\gamma_{I_2}}{8\pi^2 r_{12}^5}\frac{B_0^2}{15\mu_0 kT}\left[\chi_{xx}(3x^2-r^2)+\chi_{yy}(3y^2-r^2)+\chi_{zz}(3z^2-r^2)\right] \quad (1.69)$$

and thus, in spherical coordinates (see previous section),[41,42]

$$\Delta\nu^{\mathrm{rdc}} = -\frac{1}{4\pi}\frac{B_0^2}{15kT}\frac{\gamma_{I_1}\gamma_{I_2}\hbar}{2\pi r_{12}^3}\left[\Delta\chi_{ax}(3\cos^2\alpha-1)+\frac{3}{2}\Delta\chi_{rh}\sin^2\alpha\cos 2\beta\right] \quad (1.70)$$

where α is the angle between $\mathbf{r_{12}}$ and the z axis of the diagonal χ tensor and β is the angle which describes the position of the projection of the $\mathbf{r_{12}}$ vector on the xy plane of the χ tensor, relative to the x axis (Figure 1.3).

Eqn (1.70) has clearly the same functional form of the equation for the PCSs (eqn (1.50)); however the angles in the equation for the PCSs describe the position of the nucleus in the frame defined by the χ tensor, whereas the

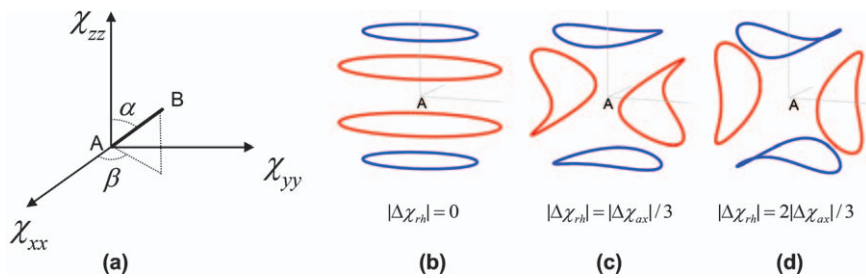

Figure 1.3 (a) Spherical coordinates defining the orientation of the coupled nuclei A and B in the frame of the χ tensor and (b)–(d) positions of the nucleus B at fixed distance from A with constant absolute RDC value (blue = positive, red = negative) for different rhombicities of the χ tensor.

angles in the equation for the RDCs describe the orientation of the vector connecting the coupled nuclei in the same reference frame. Actually, the partial self-orientation of a molecule depends on the overall $\boldsymbol{\chi}$ tensor, composed of the paramagnetic and the diamagnetic parts. However, the RDCs arising from the diamagnetic anisotropy of $\boldsymbol{\chi}$ are present also in the J measured for the diamagnetic sample, and thus, if the pRDCs are obtained from the difference in the J-couplings measured for the paramagnetic and the diamagnetic samples, the diamagnetic contribution is subtracted. In this way, only the paramagnetic contribution to the anisotropy of $\boldsymbol{\chi}$, *i.e.* the same as is responsible for the PCSs, determines the obtained pRDCs. A further contribution to the J-couplings should actually be considered, related to the presence of the dynamics frequency shift (see Section 1.5). Of note, the pRDCs, different to the PCSs, do not depend on the distance of the metal ion from the observed nuclei.

As shown for the PCSs, also the pRDCs can be calculated from the nuclear coordinates of the paramagnetic molecule and the magnetic susceptibility anisotropy tensor. The latter can be defined by (i) the five components of the anisotropic part of the symmetric $\boldsymbol{\chi}$ tensor or (ii) the two anisotropic parameters $\Delta\chi_{ax}$ and $\Delta\chi_{rh}$ and the three Euler angles describing the orientation of the main axes of the $\boldsymbol{\chi}$ tensor. In fact, the equation for the pRDCs can also be written in a generic reference frame, analogously to that of the PCSs (eqn (1.47)):

$$\Delta\nu^{\mathrm{rdc}} = -\frac{1}{4\pi}\frac{B_0^2}{15kT}\frac{3\gamma_{I_1}\gamma_{I_2}\hbar}{4\pi r_{12}^3}\Big[(\chi_{zz}-\chi_{\mathrm{iso}})(3\cos^2\alpha-1)+(\chi_{xx}-\chi_{yy})\sin^2\alpha\cos 2\beta + 2\chi_{xy}\sin^2\alpha\sin 2\beta + 2\chi_{xz}\sin 2\alpha\cos\beta + 2\chi_{yz}\sin 2\alpha\sin\beta\Big] \tag{1.71}$$

or, using the direction cosines,

$$\Delta\nu^{\mathrm{rdc}} = -\frac{1}{4\pi}\frac{B_0^2}{15kT}\frac{3\gamma_{I_1}\gamma_{I_2}\hbar}{2\pi r_{12}^3}\sum_{i,j}\chi_{ij}\cos\varphi_i\cos\varphi_j \tag{1.72}$$

where the indices i and j run over the three axes x, y and z, and φ_i are the angles between the $\mathbf{r_{12}}$ and each of the three axes. Eqn (1.72) can also be written as

$$\Delta\nu^{\mathrm{rdc}} = -\frac{1}{4\pi}\frac{B_0^2}{15kT}\frac{3\gamma_{I_1}\gamma_{I_2}\hbar}{2\pi r_{12}^5}\mathbf{r}_{\mathbf{12}}^T\cdot\boldsymbol{\chi}\cdot\mathbf{r_{12}} \tag{1.73}$$

In eqn (1.68)–(1.73) a further S_{LS} coefficient is often considered to indicate a generalized Lipari–Szabo order parameter.[43] The S_{LS} coefficient accounts for the effect of internal motions with correlation times shorter than the molecular reorientation time, and is thus able to reduce the observed pRDCs

as a result of averaging due to the multiple orientations of the $\mathbf{r_{12}}$ vector with respect to the $\boldsymbol{\chi}$ tensor.[44] Eqn (1.70), for instance, thus becomes

$$\Delta\nu^{\mathrm{rdc}} = -\frac{1}{4\pi}\frac{B_0^2}{15kT}\frac{\gamma_{I_1}\gamma_{I_2}\hbar S_{\mathrm{LS}}}{2\pi r_{12}^3}\left[\Delta\chi_{ax}(3\cos^2\alpha - 1) + \frac{3}{2}\Delta\chi_{rh}\sin^2\alpha\cos 2\beta\right] \quad (1.74)$$

The pRDCs can be used together with the PCSs as restraints in molecular structure determination[21,41,42,45] (see Figure 1.3, and Sections 3.4 and 4.2).

1.4 The Paramagnetic Relaxation Enhancements

The magnetic interaction between electron and nucleus is also responsible for a mechanism for nuclear relaxation which adds to those present in diamagnetic molecules. When the interaction is with the electron spin density localized on the nucleus, the paramagnetic enhancement is indicated as nuclear contact (or scalar) relaxation, whereas when it is with the rest of the electron spin density, it is indicated as nuclear dipolar relaxation, and it is usually treated in the point-dipole approximation.

Paramagnetic relaxation occurs because the hyperfine coupling energy (eqn (1.4) and (1.8)) fluctuates randomly with time possibly due to three mechanisms:

(i) molecular reorientation, so that the orientation of the **r** vector changes with time;
(ii) electron relaxation, so that the orientation of the **S** vector changes with time (and thus the orientation of the dipolar field generated by the electron magnetic moment to the nuclear position);
(iii) chemical exchange, so that the magnitude of the **r** vector changes with time.

The time scales for these three mechanisms are described by three correlation times, *i.e.,* the reorientation correlation time (τ_r), the electron relaxation time (τ_e) and the lifetime (τ_M), respectively.

The paramagnetic enhancements to the relaxation rates depend on the transition probabilities w_{ij} between the different states of an electron–nucleus spin system. These transition probabilities can be calculated using time-dependent perturbation theory for stochastic perturbations:[46,47]

$$w_{ij} = \frac{2}{\hbar^2}\mathrm{Re}\int_0^\infty \overline{\langle i|H_{\mathrm{hc}}(0)|j\rangle\langle j|H_{\mathrm{hc}}(t)|i\rangle}\exp(i\omega_{ij}t)\mathrm{d}t \quad (1.75)$$

where i and j indicate the eigenstates of the unperturbed Zeeman Hamiltonian, ω_{ij} is the difference between the corresponding eigenvalues divided by $\hbar$, and the bar denotes the ensemble average. In eqn (1.75) we suppose that the ensemble average is stationary, *i.e.* independent of the initial time, and that it decays to zero rapidly with respect to the integration time, so that the latter can

be extended to infinity (Redfield limit).[48–50] The transition probabilities thus depend on the autocorrelation functions defined as

$$G(t) = \overline{\langle i|H_{\rm hc}(0)|j\rangle\langle j|H_{\rm hc}(t)|i\rangle} \approx \overline{\langle i|H_{\rm hc}(0)|j\rangle^2}\exp(-t/\tau_c) \quad (1.76)$$

where it was assumed that the time-correlation function decays exponentially,[51] with the above-mentioned correlation times as the possible time constant τ_c. Finally,

$$w_{ij} = \frac{2}{\hbar^2}\mathrm{Re}\int_0^\infty \overline{\langle i|H_{\rm hc}(0)|j\rangle^2}\exp(i\omega_{ij}t - t/\tau_c)\mathrm{d}t = \frac{2\overline{\langle i|H_{\rm hc}(0)|j\rangle^2}}{\hbar^2}\frac{\tau_c}{1+\omega_{ij}^2\tau_c^2} \quad (1.77)$$

where the last term is called the Lorentzian spectral density function

$$J(\omega,\tau) = \frac{\tau}{1+\omega^2\tau^2} \quad (1.78)$$

The longitudinal and transverse relaxation rate enhancements for a nucleus in a fixed position within a paramagnetic molecule, called paramagnetic relaxation enhancements (PREs), are indicated with R_{1M} and R_{2M} ($R_{iM} = R_{iM}^{\rm dip} + R_{iM}^{\rm Curie} + R_{iM}^{\rm FC}$, see later). In the standard Solomon–Bloembergen–Morgan (SBM) model, largely used in the analysis of the relaxation rates, R_{1M} and R_{2M} are calculated from the dipolar and Fermi-contact relaxation equations as provided later in eqn (1.84), (1.85), (1.87), (1.98) and (1.99). Due to the proportionality between NMR signal linewidth and transverse relaxation rate, a paramagnetic broadening of the NMR signal occurs, equal to

$$\Delta\nu^{\rm para} = R_{2M}/\pi \quad (1.79)$$

In solutions of paramagnetic molecules, we should consider the case that the observed nucleus (for instance, the water proton) is in a ligand which may reside in two types of environment: in the coordination sphere of the paramagnetic center and in the bulk. In these cases, the longitudinal and transverse relaxation rates and the NMR shifts measured for the ligand nuclei in solution differ from the values measured in the absence of the paramagnetic center. If $R_{1\rm p}$, $R_{2\rm p}$ and $\Delta\omega_{\rm p}$ indicate the differences in relaxation rates and NMR shifts of solvent ligand nuclei between a paramagnetic solution and a diamagnetic reference solution:[52–55]

$$R_{1\rm p} = f_M(R_M^{-1} + \tau_M)^{-1} \quad (1.80)$$

$$R_{2\rm p} = \frac{f_M}{\tau_M}\frac{R_{2M}^2 + R_{2M}\tau_M^{-1} + (\Delta\omega_M)^2}{(R_{2M}+\tau_M^{-1})^2 + (\Delta\omega_M)^2} \quad (1.81)$$

$$\Delta\omega_{\rm p} = \frac{f_M}{\tau_M^2}\frac{\Delta\omega_M}{(R_{2M}+\tau_M^{-1})^2 + (\Delta\omega_M)^2} \quad (1.82)$$

where $\Delta\omega_M$ is the difference in NMR shift of the nucleus in the coordination sphere of the paramagnetic center and in a diamagnetic analogue molecule, and f_M is the mole fraction of ligand nuclei in bound positions. The chemical

exchange rate, $1/\tau_M$, of the ligand bearing the observed nucleus between bulk and coordination sphere of the paramagnetic center thus acts as a limiting factor for the propagation of the effect from the nuclei at the paramagnetic site to the bulk nuclei.

For relatively small concentrations of the paramagnetic center, the paramagnetic relaxation enhancements of solvent nuclei (sPREs) are linear with respect to the concentration of the paramagnetic center. The relaxivity r_1 is defined as the paramagnetic enhancement of the solvent nuclear relaxation rates in the presence of 0.001 mol dm^{-3} of paramagnetic centers in solution.[56] Therefore, the measured relaxation rate R_1 of the solvent nuclei can be written as

$$R_1 = R_1^{\mathrm{dia}} + R_{1\mathrm{p}} = R_1^{\mathrm{dia}} + cr_1 \tag{1.83}$$

where R_1^{dia} is the diamagnetic relaxation and c is the concentration of the paramagnetic centers. Note that R_1 in eqn (1.2) indicates the relaxation rate of a specific nucleus in the molecule, whereas in eqn (1.83) it indicates the relaxation rate of the solvent nuclei. The relationship between $R_{1\mathrm{p}}$ and R_{1M} is given in eqn (1.80).

1.4.1 Dipolar Relaxation

The paramagnetic relaxation due to the point dipole–point dipole interaction between the nuclear magnetic moment and the electron magnetic moment is traditionally split into two components, resulting from the separation of the electron spin **S** into a part **s** with zero average and the remaining part with thermal average $\mathbf{S_C}$ (see eqn (1.10)). The first term provides the Solomon equation, the second the Curie spin relaxation.

1.4.1.1 Solomon Equation

Solomon calculated the contribution to relaxation due to the dipole–dipole interaction between an electronic spin **s** with isotropic $\mathbf{g} = g_{\mathrm{e}}\mathbf{1}$ and a nuclear spin, in the hypothesis that the static Hamiltonian contains only the Zeeman interactions of the nuclear and electron magnetic moments with the external magnetic field.[46] The difference in energy in the zero quantum (w_0), single quantum (w_1) and double quantum (w_2) transitions are $\omega_S - \omega_I$, ω_I and $\omega_S + \omega_I$, respectively ($\omega_S > 0$, $\omega_I < 0$, see Figure 1.4 and eqn (1.77)) and since the electron Larmor frequency ω_S is 658.2 times larger than the nuclear Larmor frequency $|\omega_I|$ (so that $\omega_S \pm \omega_I \approx \omega_S$), it was found

$$R_{1M}^{\mathrm{dip}} = \frac{2}{15}\left(\frac{\mu_0}{4\pi}\right)^2 \frac{\gamma_I^2 g_{\mathrm{e}}^2 \mu_{\mathrm{B}}^2 S(S+1)}{r^6}\left(\frac{7\tau_{c2}^{\mathrm{dip}}}{1+\omega_S^2(\tau_{c2}^{\mathrm{dip}})^2} + \frac{3\tau_{c1}^{\mathrm{dip}}}{1+\omega_I^2(\tau_{c1}^{\mathrm{dip}})^2}\right) \tag{1.84}$$

$$R_{2M}^{\mathrm{dip}} = \frac{1}{15}\left(\frac{\mu_0}{4\pi}\right)^2 \frac{\gamma_I^2 g_{\mathrm{e}}^2 \mu_{\mathrm{B}}^2 S(S+1)}{r^6}\left(4\tau_{c1} + \frac{13\tau_{c2}^{\mathrm{dip}}}{1+\omega_S^2(\tau_{c2}^{\mathrm{dip}})^2} + \frac{3\tau_{c1}^{\mathrm{dip}}}{1+\omega_I^2(\tau_{c1}^{\mathrm{dip}})^2}\right) \tag{1.85}$$

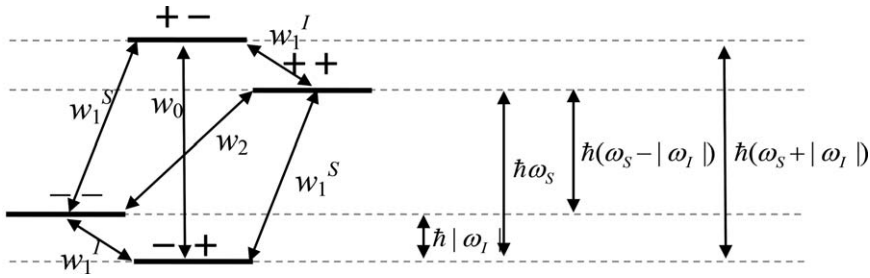

Figure 1.4 Energy levels, transition frequencies and transition probabilities in a dipole–dipole coupled *S–I* system.

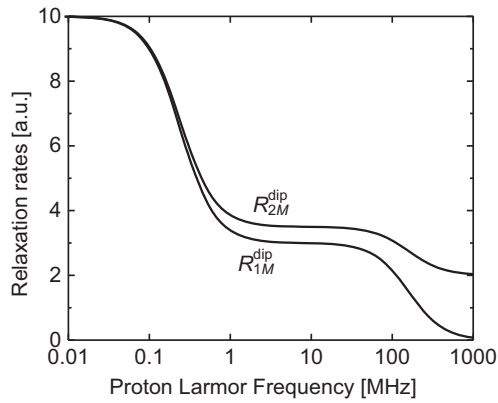

Figure 1.5 Field dependence of R_{1M}^{dip} and R_{2M}^{dip} as described by eqn (1.84) and (1.85), with a field independent $\tau_c^{dip} = 1$ ns.

The dipole–dipole interaction can be modulated by τ_r, τ_{1e}/τ_{2e} (the longitudinal/transverse electron relaxation time) and/or τ_M because each of them can contribute to the decay of the correlation function. Therefore, the correlation times are given by

$$(\tau_{c1}^{dip})^{-1} = \tau_{1e}^{-1} + \tau_r^{-1} + \tau_M^{-1}, \qquad (\tau_{c2}^{dip})^{-1} = \tau_{2e}^{-1} + \tau_r^{-1} + \tau_M^{-1} \qquad (1.86)$$

If $\tau_{1e} = \tau_{2e}$ $(= \tau_e)$, or both τ_{1e} and τ_{2e} are much larger than τ_r or τ_M, $\tau_c^{dip} = \tau_{c1}^{dip} = \tau_{c2}^{dip}$. The field dependences of the relaxation rates are shown in Figure 1.5, and are characterized by the presence of two Lorentzian dispersions centered at frequencies $\omega_S = (\tau_c^{dip})^{-1}$ and $\omega_I = (\tau_c^{dip})^{-1}$, and thus separated by a factor 658.2. In the case of lanthanoids and actinoids, the J quantum number substitutes the S quantum number and g_J substitutes g_e.

When electron relaxation is important in the definition of the correlation time, its field dependence should also be taken into account. A field dependent τ_e is expected, for instance, for all systems with $S > 1/2$ and thus possibly experiencing ZFS. Deformations of the coordination polyhedron by

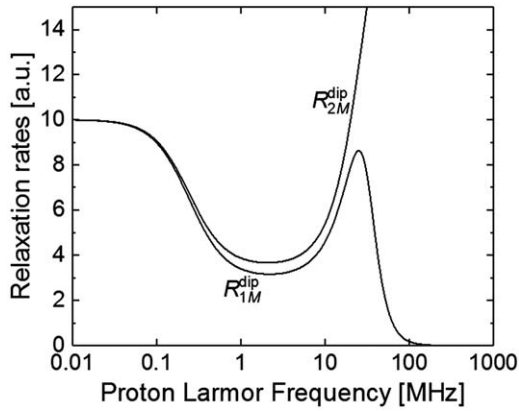

Figure 1.6 Field dependence of R_{1M}^{dip} and R_{2M}^{dip} as described by eqn (1.84) and (1.85), with a field dependent electron relaxation time, as described by eqn (1.87) (electron relaxation at low fields $\tau_{e(0)} = 1$ ns; $\tau_v = 10$ ps).

collision with solvent molecules in fact cause a transient ZFS even in high symmetry systems without static ZFS. This transient ZFS allows for the coupling of distortional motions with spin transitions and provides a relaxation mechanism for the electron(s), so that[57,58]

$$\tau_e^{-1} = \frac{2\Delta_t^2}{50}[4S(S+1) - 3]\left(\frac{\tau_v}{1+\omega_S^2\tau_v^2} + \frac{4\tau_v}{1+4\omega_S^2\tau_v^2}\right) \tag{1.87}$$

where Δ_t^2 is the mean squared fluctuation of the ZFS and τ_v is the correlation time for the instantaneous distortions of the metal coordination polyhedron. The field dependence of the nuclear longitudinal relaxation rate in the presence of field dependent electron relaxation shows a typical relaxation peak at about 1 T, due to the increase in the electron relaxation time with the increase of the field, described by eqn (1.87), and the subsequent decrease due to the $\omega_I\,\tau_c^{dip} = 1$ dispersion present in eqn (1.84) (see Figure 1.6).

Internal (intramolecular) motions can also change the **r** vector and thus be able to (at least partially) modulate the dipole–dipole interaction. In the simple Lipari–Szabo model-free treatment[43,59] (see Section 1.3), eqn (1.84) should thus be replaced by

$$R_{1M}^{dip} = \frac{2}{15}\left(\frac{\mu_0}{4\pi}\right)^2 \frac{\gamma_I^2 g_e^2 \mu_B^2 S(S+1)}{r^6}\left[S_{LS}^2\left(\frac{7\tau_c^{dip}}{1+\omega_S^2(\tau_c^{dip})^2} + \frac{3\tau_c^{dip}}{1+\omega_I^2(\tau_c^{dip})^2}\right)\right.$$
$$\left. +(1-S_{LS}^2)\left(\frac{7\tau_f^{dip}}{1+\omega_S^2(\tau_f^{dip})^2} + \frac{3\tau_f^{dip}}{1+\omega_I^2(\tau_f^{dip})^2}\right)\right] \tag{1.88}$$

where $(\tau_f^{dip})^{-1} = (\tau_c^{dip})^{-1} + \tau_l^{-1}$ and τ_l is the correlation time for the local (fast) reorientation of the nucleus-unpaired electron(s) vector. An analogous equation can be written for transverse relaxation.

1.4.1.2 Anisotropic Effects

Eqn (1.84) and (1.85) were derived by assuming (i) an isotropic electron **g** tensor and (ii) that the electron spin system is dominated by the electronic Zeeman interaction (besides the fact that reorientation, chemical exchange and electron relaxation are uncoupled and that the electron spin behaves as a point-dipole). The deviations with respect to the Solomon behaviour in the presence of an anisotropic electron **g** tensor were analyzed both in the case of fast rotation[60] and of slow rotation (with respect to the electron relaxation time)[61] and it was found that they are usually small.

In the presence of static ZFS and/or hyperfine coupling between the electron(s) and the metal nuclear magnetic moment, the energy of the nuclear and electron spin states can be very different from what is predicted using only the Zeeman term. Therefore, the energy of most electronic spin transitions can be much larger than calculated in the absence of these terms, and thus $\omega_S\tau_c$ can be much larger than one even at relatively large frequency. Furthermore, an additional dispersion in the field dependence of the relaxation rate may appear corresponding to the transition from a dominant ZFS to a dominant Zeeman energy.[62] The extent of these effects largely depends on the magnitude and rhombicity of static ZFS and/or hyperfine coupling between electron(s) and the metal nucleus, as well as on the position of the nucleus with respect to these tensors (Figure 1.7). In the so-called slow rotation limit ($\tau_r \gg \tau_e$) and within the Redfield limit, the (modified) Florence NMRD program can be used to evaluate the field dependent relaxation rates as a function of these parameters.[63–65] Outside the slow rotation limit and/or the Redfield limit, more complicated approaches should be used.[47,48,66–68]

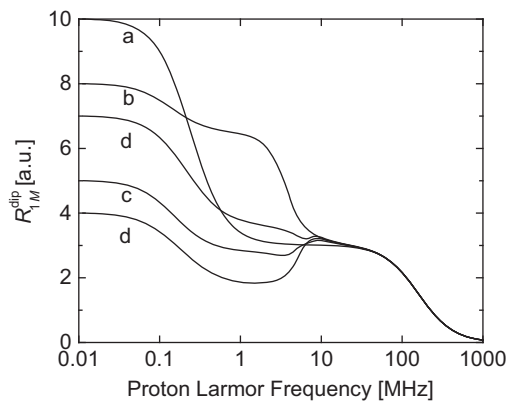

Figure 1.7 Field dependence of R_{1M}^{dip} in the absence (a) and in the presence of axial ZFS ($D = 0.1$ cm^{-1}) for a proton along the z axis (b) or in the x,y plane (c), and in the presence of ZFS with maximal rhombicity ($E/D = 1/3$, $D = 0.1$ cm^{-1}) for a proton along the z axis (d) or in the x,y plane (e) ($S = 3/2$, $\tau_c^{dip} = 1$ ns).

1.4.1.3 Outer-sphere Relaxation

In the absence of ligand molecules coordinated to the paramagnetic center, but diffusing around it, there is still a paramagnetic contribution to the relaxation of the solvent ligand nuclei. This contribution, called the outer-sphere relaxation, depends on the diffusional correlation time τ_D defined as

$$\tau_D = \frac{d^2}{D_M + D_L} \tag{1.89}$$

where d is the distance of closest approach between the ligand and the paramagnetic center, and D_M and D_L are the diffusion coefficients of the paramagnetic molecule and of the ligand molecule, respectively. Assuming that unpaired electron(s) and the ligand nucleus are in the center of hard sphere spherical molecules, according to one of the most commonly used models for diffusion[69,70]

$$R_{1p}^{OS} = \frac{32}{405}\pi\left(\frac{\mu_0}{4\pi}\right)^2 \frac{1000 N_A [M] \gamma_I^2 g_e^2 \mu_B^2 S(S+1)}{d(D_M + D_L)} [7J^{tr}(\omega_S) + 3J^{tr}(\omega_I)] \tag{1.90}$$

$$R_{2p}^{OS} = \frac{16}{405}\pi\left(\frac{\mu_0}{4\pi}\right)^2 \frac{1000 N_A [M] \gamma_I^2 g_e^2 \mu_B^2 S(S+1)}{d(D_M + D_L)} [4J^{tr}(0) + 13J^{tr}(\omega_S) + 3J^{tr}(\omega_I)] \tag{1.91}$$

where N_A is the Avogadro's constant, $[M]$ is the concentration of the paramagnetic centers, expressed in mol dm^{-3}, and the spectral density functions are given by

$$J^{tr}(\omega) = \frac{1 + 5z/8 + z^2/8}{1 + z + z^2/2 + z^3/6 + 4z^4/81 + z^5/81 + z^6/648} \tag{1.92}$$

with

$$z = (2\omega\tau_D)^{1/2} \tag{1.93}$$

or, in the case of τ_D and τ_e having comparable values,[71]

$$z = \sqrt{2\left(\omega\tau_D + \frac{\tau_D}{\tau_e}\right)}. \tag{1.94}$$

1.4.2 Curie Spin Relaxation

The paramagnetic relaxation due to the point dipole–point dipole interaction between the nuclear magnetic moment and thermal averaged electron spin $\mathbf{S}_C$ is described by the following equations (see eqn (1.56)),

$$\begin{aligned} R_{1M}^{Curie} &= \frac{2}{5}\left(\frac{\mu_0}{4\pi}\right)^2 \frac{\gamma_I^2 g_e^2 \mu_B^2 \langle S_z \rangle^2}{r^6} \frac{3\tau_c^{Curie}}{1 + \omega_I^2 (\tau_c^{Curie})^2} \\ &= \frac{2}{15}\left(\frac{\mu_0}{4\pi}\right)^2 \frac{\gamma_I^2 g_e^4 \mu_B^4 B_0^2 S^2 (S+1)^2}{k^2 T^2 r^6} \frac{\tau_c^{Curie}}{1 + \omega_I^2 (\tau_c^{Curie})^2} \end{aligned} \tag{1.95}$$

$$R_{2M}^{\text{Curie}} = \frac{1}{5}\left(\frac{\mu_0}{4\pi}\right)^2 \frac{\gamma_I^2 g_e^2 \mu_B^2 \langle S_z\rangle^2}{r^6}\left(4\tau_c + \frac{3\tau_c^{\text{Curie}}}{1+\omega_I^2(\tau_c^{\text{Curie}})^2}\right)$$
$$= \frac{1}{5}\left(\frac{\mu_0}{4\pi}\right)^2 \frac{\gamma_I^2 g_e^4 \mu_B^4 B_0^2 S^2(S+1)^2}{9k^2T^2r^6}\left(4\tau_c + \frac{3\tau_c^{\text{Curie}}}{1+\omega_I^2(\tau_c^{\text{Curie}})^2}\right) \quad (1.96)$$

where only the contribution from the single quantum (w_1) transition is present. These equations were derived assuming an isotropic **g** tensor ($\mathbf{g} = g_e\mathbf{1}$) and in the absence of ZFS and interactions of the ground S multiplet with the excited states.[72] Equations were also derived in order to consider the presence of **g** anisotropy, ZFS and/or interactions with excited states, and in these cases they contain the elements of the $\boldsymbol{\chi}$ tensor ($\mathbf{A}\cdot\mathbf{S_C} \propto \mathbf{g}\cdot\langle\mathbf{SS}\rangle\cdot\mathbf{g}^T\cdot\mathbf{B_0} \propto \boldsymbol{\chi}\cdot\mathbf{B_0}$).[73] Since in Curie spin relaxation the dipolar interaction is only with the average over all electron spin states, it can be modulated by reorientation and chemical exchange only:

$$(\tau_c^{\text{Curie}})^{-1} = \tau_r^{-1} + \tau_M^{-1} \quad (1.97)$$

In the case of lanthanoids and actinoids, the J quantum number substitutes the S quantum number and g_J substitutes g_e. Even better, the term $g_J^4\mu_B^4J^2(J+1)^2$ can be replaced with the experimental μ_{eff}^2 value, when available.[74]

Although the value of $\langle S_z\rangle^2$ is much smaller than the value of $S(S+1)/3$, which appears in the Solomon equation, Curie spin relaxation may be of the same order or larger than dipolar relaxation (eqn (1.84) and (1.85)), especially for the transverse relaxation time, when the correlation time in the Solomon equation is determined by the electron relaxation time because it is much smaller than the reorientation time. Furthermore, Curie spin relaxation increases with the square of the magnetic field, *i.e.* of the nuclear Larmor frequency $\omega_I = \gamma_I B_0$.

1.4.3 Fermi-contact Relaxation

In the case of relaxation by contact coupling, only the contribution from the zero quantum (w_0) transition is present and the relaxation rates, when $\mathbf{g} = g_e\mathbf{1}$ and in the absence of ZFS and coupling of the ground state with excited states, are equal to[75]

$$R_{1M}^{\text{FC}} = \frac{2}{3}S(S+1)\left(\frac{A^{\text{FC}}}{\hbar}\right)^2 \frac{\tau_c^{\text{FC}}}{1+\omega_S^2(\tau_c^{\text{FC}})^2} \quad (1.98)$$

$$R_{2M}^{\text{FC}} = \frac{1}{3}S(S+1)\left(\frac{A^{\text{FC}}}{\hbar}\right)^2 \left(\tau_c^{\text{FC}} + \frac{\tau_c^{\text{FC}}}{1+\omega_S^2(\tau_c^{\text{FC}})^2}\right) \quad (1.99)$$

The field dependence of the contact relaxation rates is characterized by a single Lorentzian dispersion centered at frequency $\omega_S = (\tau_c^{\text{FC}})^{-1}$ (Figure 1.8). In this case, reorientation cannot modulate the contact coupling, and thus

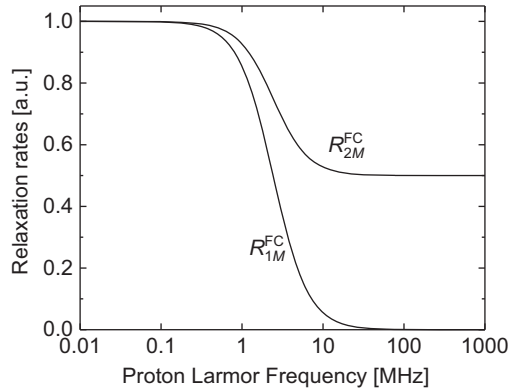

Figure 1.8 Field dependence of R_{1M}^{FC} and R_{2M}^{FC} as described by eqn (1.98) and (1.99), with an electron relaxation $\tau_e = 100$ ps.

only chemical exchange and electron relaxation can determine the correlation time, so that

$$(\tau_c^{FC})^{-1} = \tau_e^{-1} + \tau_M^{-1} \tag{1.100}$$

In the presence of possible internal (intramolecular) reorientation with correlation time τ_l able to change the electron spin density on the nucleus, contributions from spectral density functions containing the correlation time

$$(\tau_c^{FC})^{-1} = \tau_e^{-1} + \tau_M^{-1} + \tau_l^{-1} \tag{1.101}$$

may also be present and accounted for with the Lipari–Szabo model-free approach[43] (see Section 1.4.1.1).

In theory, Curie spin relaxation may also occur through contact coupling. Since Curie spin relaxation requires a correlation time much larger than the electron relaxation time $\tau_c^{FC(Curie)} = \tau_M$ and thus (for $\omega_S \tau_M \gg 1$), using eqn (1.56),

$$R_{2M}^{FC} = \langle S_z \rangle^2 \left(\frac{A^{FC}}{\hbar}\right)^2 \tau_M = \left(\frac{g_e \mu_B B_0 S(S+1)}{3kT} \frac{A^{FC}}{\hbar}\right)^2 \tau_M \tag{1.102}$$

where the term in parenthesis is related to the contact shift. Again, possible contributions arising with $(\tau_M^{-1} + \tau_l^{-1})^{-1}$ instead of τ_M should be considered in the presence of intramolecular motions.

1.5 Paramagnetic Cross Correlation Effects

Cross correlation effects arise in the presence of two (or more) different types of interactions modulated by the same motion. This results in an interference between the two interactions, related to the fact that the transition probabilities contain the square of the expectation value of all time-dependent Hamiltonian terms (in eqn (1.77) only H_{hc} is indicated), which differs from the sum of the squares of the single terms. In paramagnetic systems, one of the most important cross correlation effects is that arising in the presence of

dipole–dipole interaction between the magnetic moments of two nuclei and the dipole–dipole interaction between the magnetic moment of one nucleus and the average electron magnetic moment (responsible for Curie spin relaxation). Both of these interactions can in fact be modulated by the reorientation correlation time. In contrast, when electron relaxation is faster than molecular reorientation, there is no cross correlation arising from the dipole–dipole interaction between the magnetic moments of two nuclei and the dipole–dipole interaction between the magnetic moment of one nucleus and the electron magnetic moment (responsible for Solomon relaxation).

The cross term either decreases or increases the relaxation rates, depending on S being in the 1/2 or $-1/2$ spin state, and this causes a difference in nuclear linewidths.[76] This difference for, *e.g.*, the two proton dimension components of the HN doublet in HSQC spectra of ^{15}N enriched paramagnetic proteins, calculated in the assumption of isotropic χ tensor, is given by[76–79]

$$\Delta\nu_{1/2} = \frac{2}{15\pi}\left(\frac{\mu_0}{4\pi}\right)^2 \frac{B_0\gamma_H^2\gamma_N\mu_B^2 g_e^2\hbar S(S+1)}{r^3 r_{HN}^3 kT}\frac{3\cos^2\theta_{MHN}-1}{2}\left(4\tau_c + \frac{3\tau_c}{1+\omega_I^2\tau_c^2}\right)$$
$$= \frac{\mu_0}{4\pi}\frac{B_0\gamma_H^2\gamma_N\hbar\chi_{iso}}{10\pi^2 r^3 r_{HN}^3}\frac{3\cos^2\theta_{MHN}-1}{2}\left(4\tau_c + \frac{3\tau_c}{1+\omega_I^2\tau_c^2}\right). \quad (1.103)$$

The angle θ_{MHN} is that between the HN axis and the H-metal axis, and τ_c is the correlation time modulating both relaxation processes. Eqn (1.103) can also be generalized to treat the case of anisotropic magnetic susceptibility.[80]

The imaginary part of the cross correlation term causes a dynamic frequency shift,[51] which results in a change of the position of the individual lines of a multiplet. This effect sums to the effect arising in the presence of partial self-orientation (called RDCs, see Section 1.3, which in general can have both a diamagnetic and a paramagnetic origin), so that

$$^1J_{12}(B_0) = {}^1J_{12} + \Delta\nu^{dia} + \Delta\nu^{rdc} + \Delta\nu^{dfs} \quad (1.104)$$

and[79]

$$\Delta\nu^{dfs} = \frac{2}{5\pi}\left(\frac{\mu_0}{4\pi}\right)^2 \frac{B_0\gamma_H^2\gamma_N g_e^2\mu_B^2\hbar S(S+1)}{r_{HN}^3 r^3 kT}\frac{3\cos^2\theta_{MHN}-1}{2}\frac{\omega_I\tau_c^2}{1+\omega_I^2\tau_c^2} \quad (1.105)$$

For large correlation times and/or at high magnetic fields, the dynamic frequency shift is independent of the value of the correlation time, of the nucleus observed, and of the magnetic field, as $\frac{B_0\gamma_H^2\gamma_N\omega_I\tau_c^2}{1+\omega_I^2\tau_c^2} \approx \gamma_H\gamma_N$. The magnitude of $\Delta\nu^{dfs}$ is usually very small with respect to the paramagnetic line broadening and pRDCs.

Also the interference between Curie and CSA relaxation causes a cross correlation effect,[81] which results in decreased or increased nuclear relaxation rates depending on the relative orientation of the principal axes of CSA and

shielding tensors. The magnitude of this cross correlation effect is also usually very small, unless the Curie spin is so large that paramagnetic relaxation is predominantly due to the Curie rather than the dipolar contribution.

1.6 First Principles Calculation of Hyperfine Shifts

In quantum chemistry computations, the $\mathbf{A}^{\mathbf{DIP}}$ tensor, in the non-relativistic approximation, refers to the interaction between the electron spin magnetic moment, without considering the orbital contributions, and the nuclear magnetic moment, so that[6]

$$\mathbf{A}^{\mathbf{DIP}} = \frac{\mu_0}{4\pi}\frac{\hbar\gamma_I\mu_B g_e}{r^3}\left(\frac{3\mathbf{rr}}{r^2} - \mathbf{1}\right) \tag{1.106}$$

If $\mathbf{g}$ is separated into $(g_e + \Delta g_{iso})\mathbf{1} + \mathbf{\Delta g}$, the contact shift (see eqn (1.35) and (1.36)) is split into two components ($g_e A^{FC}\langle\mathbf{SS}\rangle$ and $\Delta g_{iso}A^{FC}\langle\mathbf{SS}\rangle$) with non-null isotropic average and one traceless component ($A^{FC}\mathbf{\Delta g}\cdot\langle\mathbf{SS}\rangle$).[4,8,82] The electron spin–nuclear spin dipole–dipole shift (see eqn (1.42) and (1.43)) is provided by the term $\mathbf{\Delta g}\cdot\langle\mathbf{SS}\rangle\cdot\mathbf{A}^{\mathbf{DIP}}$, the trace of which can be different from zero, thus providing a non-null isotropic average. Further traceless anisotropic components are provided by the terms $g_e\langle\mathbf{SS}\rangle\cdot\mathbf{A}^{\mathbf{DIP}}$ and $\Delta g_{iso}\langle\mathbf{SS}\rangle\cdot\mathbf{A}^{\mathbf{DIP}}$, as well as by spin–orbit correction terms.[4,8,82] The spin–orbit correction provides three further components of the hyperfine coupling tensor, namely the spin–orbit contribution to the isotropic hyperfine coupling constant and to the hyperfine anisotropy, and an anti-symmetric spin–orbit contribution.[83] All together these terms, however, do not recover the interaction between the orbital magnetic moment and the nuclear magnetic moment, as described in Kurland and McGarvey.[3]

First principles calculations of the hyperfine shifts require the evaluation of the $\mathbf{g}$, $\mathbf{D}$ (ZFS, for $S > 1/2$) and $\mathbf{A}$ tensors by taking into account all thermally accessible energy levels of the electron spin states. In the point-dipole approximation, the electron spin–nuclear spin dipole–dipole shifts can be predicted from the molecular structure after calculation of the $\mathbf{g}$ and $\mathbf{D}$ tensors ($\mathbf{D}$ is needed to calculate $\langle\mathbf{SS}\rangle$). Contact shifts require the determination of $\mathbf{g}$, $\langle\mathbf{SS}\rangle$ and A^{FC} (see eqn (1.36)). Of course, an accurate treatment of spin–orbit coupling is necessary for $\mathbf{g}$ tensor calculations. Whereas the hyperfine coupling tensor can be calculated using density-functional theory (DFT), in several cases DFT is inaccurate for the evaluation of the $\mathbf{D}$ tensor and the $\mathbf{g}$ tensor.[84–86] These tensors can be better estimated using multi-reference wavefunction theories (WFT) at the complete active space self-consistent field (CASSCF) and n-electron valence state perturbation theory 2 (NEVPT2) levels,[4] and a molecular model comprising the nuclei in closest proximity to the paramagnetic center. Using this approach, the electron spin–nuclear spin dipole–dipole shifts were calculated for the nuclei of a high-spin cobalt(II) protein from its crystal structure, and were found in agreement with experimental PCSs.[35] The contribution to the PCSs from the dipole–dipole interaction between electron orbital magnetic moment and nuclear magnetic

moment is likely masked by inaccuracies in the calculation of the D tensor, also arising from possible slight inaccuracies in the protein structural model.

In the absence of ZFS, DFT calculations of hyperfine coupling constants, **g** tensor and orbital shieldings gave accurate enough results to provide contact shifts in good agreement with the experimental data, for instance, for nitroxide radicals,[82,87] chromium(III), manganese(III), iron(III), and copper(II) acetylacetonates, with the metal ions in the high spin states (Cr: $S = 3/2$, Mn: $S = 2$, Fe: $S = 5/2$, Cu: $S = 1/2$),[87] after geometry optimization of a structural model at the B3LYP/cc-pVTZ level, and for paramagnetic iron–sulfur proteins, as in the case of iron(III) rubredoxin.[88]

1.7 Metal Ion Dependence of the Paramagnetic Effects

The key parameters determining the magnitude of PCSs, pRDCs and PREs are the magnetic susceptibility anisotropy and the electron relaxation time.[89] Metal ions with very low paramagnetic susceptibility anisotropy are gadolinium(III), manganese(II), and type-2 copper(II). Therefore, they produce very small (usually undetectable) PCSs and pRDCs. On the other hand, these metal ions have a long electron relaxation time, which induces relatively large PREs (see Table 1.1 and Figure 1.9). In fact, in macromolecules with large reorientation time, the correlation time τ_c is often determined by the electron relaxation time. As is clear from eqn (1.85), the larger τ_c, the larger R_{2M}, and thus the paramagnetic broadening of the observed NMR signals. The PREs may make the signals of nuclei relatively close to the metal so broad as to be undetectable.

Metal ions with short electron relaxation times, in contrast, determine small PREs (if Curie spin relaxation can be neglected) and thus a small broadening of the NMR lines, so that the quality of the NMR spectra of the diamagnetic analogues is preserved. This is the case of low-spin iron(III), high-spin iron(II), titanium(III), nickel(II), cobalt(II) and type-1 copper(II). Most of these also have a relatively small, but still sizable, paramagnetic susceptibility anisotropy, so that PCSs can be measured. High spin iron(III) has a paramagnetic susceptibility anisotropy of similar magnitude, but PCSs and pRDCs can hardly be observed in large macromolecules due to the occurrence of Curie spin relaxation.

Paramagnetic lanthanoid(III) ions except gadolinium(III) may have paramagnetic susceptibility anisotropies from small to very large (see Section 2.2.2).[90–92] They also have electron relaxation times smaller than 10^{-12} s. However, the R_{2M} in lanthanoid(III) macromolecules, and thus the paramagnetic line broadening, can be very large due to Curie spin relaxation (which also depends on J and g_J). Paramagnetic lanthanoid(III) ions with large paramagnetic susceptibility anisotropy are terbium(III), dysprosium(III), thulium(III) and holmium(III). They thus produce large PCSs and pRDCs outside the large blind region of these metal ions, where no signal

Table 1.1 Values of the magnetic susceptibility per molecule, as calculated with eqn (1.58) at $T = 298$ K, and typical values of the electron relaxation time at high fields and of the axial anisotropy of the paramagnetic susceptibility tensors for the different paramagnetic metal ions.

	g_e/g_J	S/J	τ_e [ps]	χ [10^{-32} m^3]	$\lvert\Delta\chi_{ax}\rvert$ [10^{-32} m^3]
Ti(III)	2.0	1/2	40	2.6	0.4
VO^{2+}	2.0	1/2	500–2000	2.6	0.1
Cr(III)	2.0	3/2	1000	13	<0.1
Mn(II)	2.0	5/2	10 000	31	<0.1
Mn(III), high spin	2.0	2	50	21	0.5
Fe(III), high spin	2.0	5/2	10–1000	31	0.6–3
Fe(III), low spin	2.0	1/2	1	2.6	2.4
Fe(II), high spin	2.0	2	1	21	2.1
Co(II), high spin, hexacoord.	2.0	3/2	1	13	7
Co(II), high spin, tetracoord.	2.0	3/2	10	13	3
Co(II), low spin	2.0	1/2	100	2.6	1
Ni(II), hexacoord.	2.0	1	100	7	2
Ni(II), tetracoord.	2.0	1	1	7	1.5
Type-1 Cu(II)	2.0	1/2	500	2.6	0.6
Type-2 Cu(II)	2.0	1/2	3000	2.6	0.6
Ce(III)	6/7	5/2	0.1	5.6	2
Pr(III)	4/5	4	0.1	11	3.5
Nd(III)	8/11	9/2	0.2	11	1.7
Sm(III)	2/7	5/2	0.1	0.6	0.2
Eu(III)	—	0[a]	0.01	0[a]	2.4
Gd(III)	2.0	7/2	10 000	55	0.2
Tb(III)	3/2	6	0.3	83	40
Dy(III)	4/3	15/2	0.5	99	35
Ho(III)	5/4	8	0.3	99	20
Er(III)	6/5	15/2	0.3	80	12
Tm(III)	7/6	6	0.5	50	25
Yb(III)	8/7	7/2	0.3	18	8

[a]Eu(III) is paramagnetic due to the excited states.

can be detected due to the very large line broadening. Cerium(III), neodymium(III) and europium(III) have a much smaller paramagnetic susceptibility anisotropy, and also a smaller Curie spin relaxation, and erbium(III) and ytterbium(III) are characterized by intermediate values.

1.8 The Overhauser Effect in Paramagnetic Systems

The nuclear Overhauser effect (NOE) is the result of the transfer of spin population (called polarization transfer) between two nuclei which are dipole–dipole coupled, upon irradiation of one of the nuclei. When the equilibrium population of the two energy levels (with different spin state) of one nucleus is altered by radiofrequency irradiation at the frequency corresponding to the transition between the two spin states, also the population of the second,

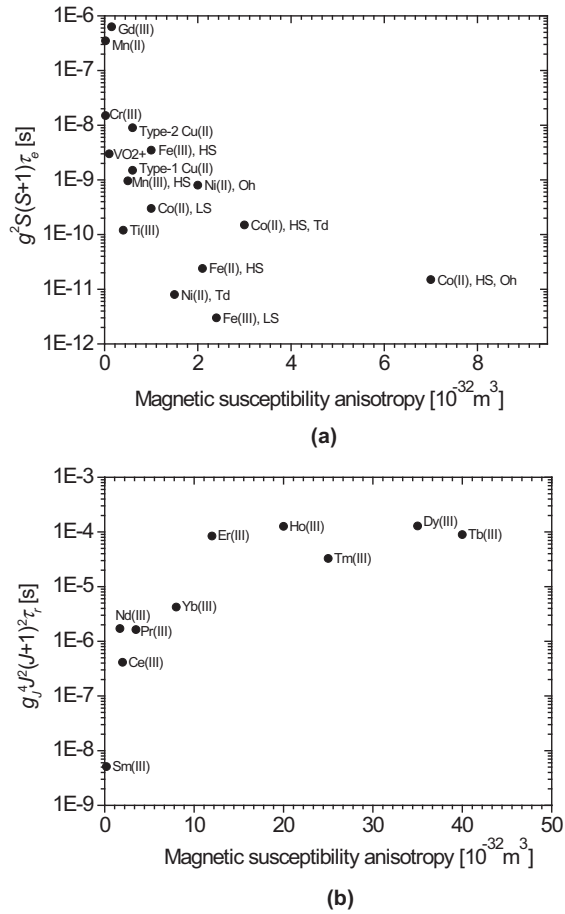

Figure 1.9 Typical values of $g^2S(S+1)\tau_e$ (on which the paramagnetic relaxation and line broadening—in the absence of Curie-spin relaxation—depend) and of the axial paramagnetic susceptibility anisotropy (on which PCSs and pRDCs depend) for paramagnetic transition metal ions (a). In lanthanoid(III) ions except gadolinium (b), relaxation is dominated by the Curie spin relaxation, which depends on $g_J^4J^2(J+1)^2\tau_r$ ($\tau_r = 10$ ns, HS = high spin, LS = low spin, Oh = octahedral geometry, Td = tetrahedral geometry).

dipole–dipole coupled nucleus is perturbed. Therefore, selective irradiation of one signal produces a change in the intensity in the other signal.

If the nuclear spin **I** is observed, and the dipole–dipole coupled nuclear spin **J** is saturated for a time long enough that the system reaches a new steady state equilibrium, the steady state NOE $\eta_{I(J)}$ is given by

$$\eta_{I(J)} = \frac{\sigma_{I(J)}}{\rho_I}\frac{J(J+1)\gamma_J}{I(I+1)\gamma_I} \tag{1.107}$$

where ρ_I represents the longitudinal relaxation rate of spin **I** and $\sigma_{I(J)}$ is called the cross-relaxation rate

$$\sigma_{I(J)} = w_2 - w_0 = \left(\frac{\mu_0}{4\pi}\right)^2 \frac{2\hbar^2\gamma_I^2\gamma_J^2 J(J+1)}{15r_{IJ}^6}\left[\frac{6\tau_c}{1+(\omega_I+\omega_J)^2\tau_c^2} - \frac{\tau_c}{(1+(\omega_I-\omega_J)^2\tau_c^2}\right] \quad (1.108)$$

The nucleus **I** is coupled to the nucleus **J** and to many other nuclei. In paramagnetic systems, the nucleus **I** is also coupled to the paramagnetic center, so that ρ_I is the sum of the contributions arising from all these interactions:

$$\rho_I = \rho_{I(J)} + \rho_{I(\text{other})} + R_{1M}^I \quad (1.109)$$

where $\rho_{I(J)}$ represents the contribution to the longitudinal relaxation rate of spin **I** due to the interaction with spin **J** upon reciprocal reorientation (see Section 1.4.1.1)

$$\rho_{I(J)} = w_0 + 2w_1^I + w_2 = \left(\frac{\mu_0}{4\pi}\right)^2 \frac{2\hbar^2\gamma_I^2\gamma_J^2 J(J+1)}{15r_{IJ}^6} \times \left[\frac{\tau_c}{1+(\omega_I-\omega_J)^2\tau_c^2} + \frac{3\tau_c}{1+\omega_I^2\tau_c^2} + \frac{6\tau_c}{1+(\omega_I+\omega_J)^2\tau_c^2}\right] \quad (1.110)$$

and R_{1M}^I is its paramagnetic relaxation rate. Therefore, the homonuclear NOE is

$$\eta_{I(J)} = \frac{\sigma_{I(J)}}{\rho_{I(J)} + \rho_{I(\text{other})} + R_{1M}^I} \quad (1.111)$$

Of course, the larger the denominator in eqn (1.111), the smaller the NOE. Therefore, when the R_{1M} term is larger than the other terms, relaxation can be very effective and the NOE very small.

Acknowledgements

The support from Fondazione Cassa di Risparmio di Firenze, MIUR PRIN 2012SK7ASN, European Commission project pNMR No. 317127, and Instruct-ERIC, a Landmark ESFRI project, is acknowledged. Discussions with Ladislav Benda, Martin Kaupp, Jozef Kowalewski, Jiři Mareš, Guido Pintacuda and Juha Vaara are acknowledged.

References

1. I. Bertini, C. Luchinat, G. Parigi and E. Ravera, *NMR of Paramagnetic Molecules: Applications to Metallobiomolecules and Models*, 2017.

2. H. M. McConnell and R. E. Robertson, *J. Chem. Phys.*, 1958, **29**, 1361–1365.
3. R. J. Kurland and B. R. McGarvey, *J. Magn. Reson.*, 1970, **2**, 286–301.
4. S. A. Rouf, J. Mareš and J. Vaara, *J. Chem. Theory Comput.*, 2015, **11**, 1683–1691.
5. I. Bertini, C. Luchinat and G. Parigi, *Prog. Nucl. Magn. Reson. Spectrosc.*, 2002, **40**, 249–273.
6. *Calculation of NMR and EPR Parameters: Theory and Applications*, ed. M. Kaupp, M. Bühl and V. G. Malkin, Wiley-VCH, Weinheim, 2004.
7. A. Soncini and W. Van den Heuvel, *J. Chem. Phys.*, 2013, **138**, 021103.
8. T. O. Pennanen and J. Vaara, *Phys. Rev. Lett.*, 2008, **100**, 133002.
9. W. Van den Heuvel and A. Soncini, *Phys. Rev. Lett.*, 2012, **109**, 073001.
10. J. Vaara, S. A. Rouf and J. Mareš, *J. Chem. Theory Comput.*, 2015, **11**, 4840–4849.
11. I. Bertini, C. Luchinat and G. Parigi, *Eur. J. Inorg. Chem.*, 2000, 2473–2480.
12. M. Karplus, *J. Am. Chem. Soc.*, 1963, **85**, 2870–2871.
13. I. Bertini, F. Capozzi, C. Luchinat, M. Piccioli and A. J. Vila, *J. Am. Chem. Soc.*, 1994, **116**, 651–660.
14. I. Bertini, S. Ciurli, A. Dikiy, R. Gasanov, C. Luchinat, G. Martini and N. Safarov, *J. Am. Chem. Soc.*, 1999, **121**, 2037–2046.
15. I. Bertini, C. Luchinat, G. Parigi and F. A. Walker, *J. Biol. Inorg. Chem.*, 1999, **4**, 515–519.
16. I. Bertini, A. Dikiy, C. Luchinat, R. Macinai and M. S. Viezzoli, *Inorg. Chem.*, 1998, **37**, 4814–4821.
17. E. A. Suturina and I. Kuprov, *Phys. Chem. Chem. Phys.*, 2016, **18**, 26412–26422.
18. I. Bertini, C. Luchinat and G. Parigi, *Concepts Magn. Reson.*, 2002, **14**, 259–286.
19. I. Bertini, P. Kursula, C. Luchinat, G. Parigi, J. Vahokoski, M. Willmans and J. Yuan, *J. Am. Chem. Soc.*, 2009, **131**, 5134–5144.
20. I. Bertini, C. Del Bianco, I. Gelis, N. Katsaros, C. Luchinat, G. Parigi, M. Peana, A. Provenzani and M. A. Zoroddu, *Proc. Natl. Acad. Sci. U. S. A.*, 2004, **101**, 6841–6846.
21. R. Barbieri, C. Luchinat and G. Parigi, *ChemPhysChem*, 2004, **21**, 797–806.
22. G. Pintacuda, M. John, X.-C. Su and G. Otting, *Acc. Chem. Res.*, 2007, **40**, 206–212.
23. T. Zhuang, H.-S. Lee, B. Imperiali and J. H. Prestegard, *Protein Sci.*, 2008, **17**, 1220–1231.
24. P. H. J. Keizers, A. Saragliadis, Y. Hiruma, M. Overhand and M. Ubbink, *J. Am. Chem. Soc.*, 2008, **130**, 14802–14812.
25. L. de la Cruz, T. H. D. Nguyen, K. Ozawa, J. Shin, B. Graham, T. Huber and G. Otting, *J. Am. Chem. Soc.*, 2011, **133**, 19205–19215.
26. Y. Kobashigawa, T. Saio, M. Ushio, M. Sekiguchi, M. Yokochi, K. Ogura and F. Inagaki, *J. Biomol. NMR*, 2012, **53**, 53–63.

27. H. Yagi, K. B. Pilla, A. Maleckis, B. Graham, T. Huber and G. Otting, *Structure*, 2013, **21**, 883–890.
28. L. Cerofolini, G. B. Fields, M. Fragai, C. F. G. C. Geraldes, C. Luchinat, G. Parigi, E. Ravera, D. I. Svergun and J. M. C. Teixeira, *J. Biol. Chem.*, 2013, **288**, 30659–30671.
29. J.-Y. Guan, P. H. J. Keizers, W.-M. Liu, F. Löhr, S. P. Skinner, E. A. Heeneman, H. Schwalbe, M. Ubbink and G. Siegal, *J. Am. Chem. Soc.*, 2013, **135**, 5859–5868.
30. M. Rinaldelli, E. Ravera, V. Calderone, G. Parigi, G. N. Murshudov and C. Luchinat, *Acta Crystallogr., Sect. D: Biol. Crystallogr.*, 2014, **70**, 958–967.
31. D. J. Crick, J. X. Wang, B. Graham, J. D. Swarbrick, H. R. Mott and D. Nietlispach, *J. Biomol. NMR*, 2015, **61**, 197–207.
32. A. Carlon, E. Ravera, W. Andrałojć, G. Parigi, G. N. Murshudov and C. Luchinat, *Prog. Nucl. Magn. Reson. Spectrosc.*, 2016, **92–93**, 54–70.
33. M. Rinaldelli, A. Carlon, E. Ravera, G. Parigi and C. Luchinat, *J. Biomol. NMR*, 2015, **61**, 21–34.
34. B. J. Walder, K. K. Dey, M. C. Davis, J. H. Baltisberger and P. J. Grandinetti, *J. Chem. Phys.*, 2015, **142**, 014201.
35. L. Benda, J. Mareš, E. Ravera, G. Parigi, C. Luchinat, M. Kaupp and J. Vaara, *Angew. Chem., Int. Ed. Engl.*, 2016, **55**, 14713–14717.
36. G. T. P. Charnock and I. Kuprov, *Phys. Chem. Chem. Phys.*, 2014, **16**, 20184–20189.
37. H. M. McConnell and D. B. Chesnut, *J. Chem. Phys.*, 1958, **28**, 107–117.
38. I. Bertini, I. C. Felli and C. Luchinat, *J. Magn. Reson.*, 1998, **134**, 360–364.
39. M. John, A. Y. Park, G. Pintacuda, N. E. Dixon and G. Otting, *J. Am. Chem. Soc.*, 2005, **127**, 17190–17191.
40. C. Schmitz, M. J. Stanton-Cook, X.-C. Su, G. Otting and T. Huber, *J. Biomol. NMR*, 2008, **41**, 179–189.
41. J. R. Tolman, J. M. Flanagan, M. A. Kennedy and J. H. Prestegard, *Proc. Natl. Acad. Sci. U. S. A.*, 1995, **92**, 9279–9283.
42. L. Banci, I. Bertini, J. G. Huber, C. Luchinat and A. Rosato, *J. Am. Chem. Soc.*, 1998, **120**, 12903–12909.
43. G. Lipari and A. Szabo, *J. Am. Chem. Soc.*, 1982, **104**, 4546–4559.
44. M. Fragai, C. Luchinat, G. Parigi and E. Ravera, *Coord. Chem. Rev.*, 2013, **257**, 2652–2667.
45. S. Balayssac, I. Bertini, C. Luchinat, G. Parigi and M. Piccioli, *J. Am. Chem. Soc.*, 2006, **128**, 15042–15043.
46. I. Solomon, *Phys. Rev.*, 1955, **99**, 559–565.
47. J. Kowalewski and L. Maler, *Nuclear Spin Relaxation in Liquids: Theory, Experiments, and Applications*, Taylor & Francis, 2006.
48. J. Kowalewski, D. Kruk and G. Parigi, *Adv. Inorg. Chem.*, 2005, **57**, 41–104.
49. M. Goldman, *J. Magn. Reson.*, 2001, **149**, 160–187.
50. C. P. Slichter, *Principles of Magnetic Resonance*, Springer, Berlin, 1992.
51. A. Abragam, *The Principles of Nuclear Magnetism*, Oxford University Press, Oxford, 1961.

52. J. S. J. Leigh, *J. Magn. Reson.*, 1971, **4**, 308–311.
53. T. J. Swift and R. E. Connick, *J. Chem. Phys.*, 1962, **37**, 307–320.
54. A. C. McLaughlin and J. S. Leigh, *J. Magn. Reson.*, 1973, **9**, 296–304.
55. G. N. La Mar, W. D. Horrocks and R. H. Holm, *NMR of Paramagnetic Molecules: Principles and Applications*, Elsevier Science, Burlington, 2013.
56. I. Bertini, C. Luchinat and G. Parigi, *Adv. Inorg. Chem.*, 2005, **57**, 105–172.
57. N. Bloembergen and L. O. Morgan, *J. Chem. Phys.*, 1961, **34**, 842–850.
58. M. Rubinstein, A. Baram and Z. Luz, *Mol. Phys.*, 1971, **20**, 67–80.
59. P. Caravan, N. J. Cloutier, S. A. McDermid, J. J. Ellison, J. M. Chasse, R. B. Lauffer, C. Luchinat, T. J. McMurry, G. Parigi and M. Spiller, *Inorg. Chem.*, 2007, **46**, 6632–6639.
60. H. Sternlicht, *J. Chem. Phys.*, 1965, **42**, 2250–2251.
61. I. Bertini, C. Luchinat and K. V. Vasavada, *J. Magn. Reson.*, 1990, **89**, 243–254.
62. I. Bertini, O. Galas, C. Luchinat, L. Messori and G. Parigi, *J. Phys. Chem.*, 1995, **99**, 14217–14222.
63. I. Bertini, O. Galas, C. Luchinat and G. Parigi, *J. Magn. Reson., Ser. A*, 1995, **113**, 151–158.
64. I. Bertini, J. Kowalewski, C. Luchinat, T. Nilsson and G. Parigi, *J. Chem. Phys.*, 1999, **111**, 5795–5807.
65. D. Kruk, T. Nilsson and J. Kowalewski, *Phys. Chem. Chem. Phys.*, 2001, **3**, 4907–4917.
66. T. Larsson, P. O. Westlund, J. Kowalewski and S. H. Koenig, *J. Chem. Phys.*, 1994, **101**, 1116–1128.
67. P. H. Fries and E. Belorizky, *J. Chem. Phys.*, 2007, **126**, 204503.
68. S. Rast, P. H. Fries, E. Belorizky, A. Borel, L. Helm and A. E. Merbach, *J. Chem. Phys.*, 2001, **115**, 7554–7563.
69. L. P. Hwang and J. H. Freed, *J. Chem. Phys.*, 1975, **63**, 4017–4025.
70. C. F. Polnaszek and R. G. Bryant, *J. Chem. Phys.*, 1984, **81**, 4038–4045.
71. J. H. Freed, *J. Chem. Phys.*, 1978, **68**, 4034–4037.
72. M. Gueron, *J. Magn. Reson.*, 1975, **19**, 58–66.
73. A. J. Vega and D. Fiat, *Mol. Phys.*, 1976, **31**, 347–355.
74. C. Vigouroux, E. Belorizky and P. H. Fries, *Eur. Phys. J. D*, 1999, **5**, 243–255.
75. N. Bloembergen, *J. Chem. Phys.*, 1957, **27**, 575–596.
76. I. Bertini, C. Luchinat, M. Piccioli and D. Tarchi, *Concepts Magn. Reson.*, 1994, **6**, 307–335.
77. M. Goldman, *J. Magn. Reson.*, 1984, **60**, 437–452.
78. I. Bertini, C. Luchinat and D. Tarchi, *Chem. Phys. Lett.*, 1993, **203**, 445–449.
79. R. Ghose and J. H. Prestegard, *J. Magn. Reson.*, 1997, **128**, 138–143.
80. I. Bertini, J. Kowalewski, C. Luchinat and G. Parigi, *J. Magn. Reson.*, 2001, **152**, 103–108.
81. G. Pintacuda, A. Kaikkonen and G. Otting, *J. Magn. Reson.*, 2004, **171**, 233–243.
82. M. Kaupp and F. H. Köhler, *Coord. Chem. Rev.*, 2009, **253**, 2376–2386.

83. A. V. Arbuznikov, J. Vaara and M. Kaupp, *J. Chem. Phys.*, 2004, **120**, 2127–2139.
84. F. Neese, *J. Chem. Phys.*, 2007, **127**, 164112.
85. O. L. Malkina, J. Vaara, B. Schimmelpfennig, M. Munzarová, V. G. Malkin and M. Kaupp, *J. Am. Chem. Soc.*, 2000, **122**, 9206–9218.
86. A. Kubica, J. Kowalewski, D. Kruk and M. Odelius, *J. Chem. Phys.*, 2013, **138**, 064304.
87. F. Rastrelli and A. Bagno, *Chem. – Eur. J.*, 2009, **15**, 7990–8004.
88. S. J. Wilkens, B. Xia, F. Weinhold, J. L. Markley and W. M. Westler, *J. Am. Chem. Soc.*, 1998, **120**, 4806–4814.
89. I. Bertini, C. Luchinat, G. Parigi and R. Pierattelli, *ChemBioChem*, 2005, **6**, 1536–1549.
90. B. Bleaney, *J. Magn. Reson.*, 1972, **8**, 91–100.
91. I. Bertini, M. B. L. Janik, Y.-M. Lee, C. Luchinat and A. Rosato, *J. Am. Chem. Soc.*, 2001, **123**, 4181–4188.
92. I. Bertini, A. Donaire, B. Jiménez, C. Luchinat, G. Parigi, M. Piccioli and L. Poggi, *J. Biomol. NMR*, 2001, **21**, 85–98.